

NASA TECHNICAL NOTE



NASA TN D-5245

c. 1

NASA TN D-5245



**LOAN COPY: RETURN TO
AFWL (WLIL-2)
KIRTLAND AFB, N MEX**

**UNACCELERATED GEOCENTRIC
VELOCITIES AND INFLUX RATES
OF SPORADIC PHOTOGRAPHIC METEORS**

by C. D. Miller

Lewis Research Center

Cleveland, Ohio



UNACCELERATED GEOCENTRIC VELOCITIES
AND INFLUX RATES OF SPORADIC
PHOTOGRAPHIC METEORS

By C. D. Miller

Lewis Research Center
Cleveland, Ohio

NATIONAL AERONAUTICS AND SPACE ADMINISTRATION

For sale by the Clearinghouse for Federal Scientific and Technical Information
Springfield, Virginia 22151 - CFSTI price \$3.00

ABSTRACT

Author's weighting factor to correct photographic bias due to mass and velocity was applied to Smithsonian data for over 2000 sporadic meteors. The factor was supported by confirmation of predicted agreement between a velocity histogram for meteors of all masses obtained with its use and a raw distribution for large masses. An equation was found for geocentric velocity distribution unaccelerated by Earth gravity. Exponent of mass of 1.34 was obtained in equation for cumulative mass distribution using mass scale of McCrosky and Posen. An average velocity of 13.8 km/sec was obtained, *virtually independent of mass.*

UNACCELERATED GEOCENTRIC VELOCITIES AND INFLUX RATES OF SPORADIC PHOTOGRAPHIC METEORS

by C. D. Miller

Lewis Research Center

SUMMARY

Use was made of an earlier published weighting factor, developed at NASA Lewis Research Center, for correction of photographic bias caused by variation in mass and velocity of meteors. The weighting factor was applied to all sporadic meteors among approximately 2400 for which photographically derived data had been published by the Smithsonian Astrophysical Observatory.

For unaccelerated geocentric velocities of meteors intersecting Earth's orbit the results indicated an average value of 13.80 kilometers per second. This value contrasts with previously estimated values ranging from 20 to 40 kilometers per second. Application of the weighting factor showed a close approximation to a log-normal geocentric velocity distribution, but with the values of probability density offset 1.5 kilometers per second upward on the velocity scale. As predicted, the weighted velocity distribution agreed closely with a raw velocity distribution for a part of the total sample of photographic meteors consisting approximately of the heaviest 10 percent. Such prediction was made on the assumptions that velocity distribution should be nearly independent of mass and that no difficulty should be encountered in photographing even the slowest meteors of very large mass. The weighted velocity distribution for all masses was also shown to agree with the raw distributions for groups of meteors of lower masses, but only for meteors above some critical velocity level at which the slowest of meteors could be easily photographed.

Comparison of semilogarithmic plots of the weighted distribution for all masses with the raw distribution for a mass group yielded a correction factor by which the actual count of meteors within the mass group could be multiplied to compensate for the failure to photograph slower meteors. By use of such correction factors, a corrected distribution of mass influx rates was obtained. Such distribution proved to be a straight line on a full logarithmic plot at least down to a mass of 0.02 gram. The slope of the line and its level, perhaps fortuitously, agreed with earlier values within the probable accuracy of the method.

The previously developed weighting factor is believed to be well supported by the correlations it produces.

INTRODUCTION

A part of the solar system about which existing knowledge is quite limited is a vast number of sporadic meteoroids. More extensive knowledge concerning them seems to be desirable, not only in keeping with the objective of increasing man's knowledge of his environment, but also because the possibility of collisions with them poses a potentially important problem in the planning of long space missions.

Meteoroids are small particles that are known to be present within the free space of the solar system and are generally in elliptic orbits about the sun. When such a particle encounters the atmosphere of Earth, it almost always possesses a velocity relative to the atmosphere at least as great as the velocity of escape from Earth (about 11 km/sec) and may have a velocity above 70 kilometers per second. If the mass of the particle is much greater than 10^{-3} gram, a trail may be created in the atmosphere sufficiently luminous to be visible as a streak across the sky. The appearance of such a luminous streak is known as a "meteor." The particle that causes it, however, is still properly termed a "meteoroid."

If such a meteoroid has an original mass as great as about 10^{-2} gram, the resulting meteor may be sufficiently luminous that it can be photographed. The mass range of so-called "photographic" meteors extends from this level of about 10^{-2} to 10 or 10^2 grams. Above the higher levels, meteors may be so rare that a sample of reasonable size might contain none, and overexposure of the photographic plate might cause reduction to be impossible.

The mass range covered by the photographic meteoroids may be of particular importance for long space missions. A meteoroid having a mass within this range could penetrate a substantial thickness of armor. Moreover, the probable frequency of encounter of such meteoroids may be great enough to represent a substantial hazard to a space vehicle or space radiator having several hundreds of square feet of vulnerable area exposed over a period of many months.

According to recent results of hypervelocity impact tests (ref. 1), the armor thickness that can be penetrated by a particle varies as the one-third power of particle mass and as the first power of impact velocity. Hence, in assessing the degree of hazard to a long-range space mission represented by meteoroids within the photographic range, it is necessary to know accurately the influx rate at each possible combination of mass and velocity. In other words, it is necessary to know the influx rate for all mass ranges and the velocity distribution within each mass range.

Determination of either influx rates for various mass ranges or velocity distribution within a mass range is complicated by a bias due to the effect of either mass or velocity on the brilliance of a meteor. Because of this biasing effect, a heavier meteoroid is more likely to result in a photographic meteor than is a lighter meteoroid, and a meteoroid

possessing a higher velocity relative to Earth atmosphere is much more likely to produce a photographic meteor than a slower meteoroid.

A recently published analysis (ref. 2) has shown that for sporadic meteors both the mass and velocity biases can be compensated by use of a weighting factor approximately proportional to the -4.22 power of the velocity of a meteoroid relative to Earth atmosphere. This factor is also a function, to a lesser extent, of the angle of meteoroid path to the zenith. In use of such weighting factor each photographic meteor is counted, not as one meteor, but as one multiplied by the weighting factor as computed from the velocity and zenith angle of that meteor. The resulting corrected counts for various velocities relative to Earth atmosphere should provide a true representation of velocity distribution for all photographic meteors of mass greater than any specified level. The weighting factor of reference 2 was first determined theoretically and then revised on an empirical basis. The empirical revision, however, agreed closely with the theoretically derived factor as to the exponent of atmospheric velocity, which, in practice, is much more important than the dependence of the weighting factor on zenith angle.

An earlier weighting factor that has been widely used for a similar purpose (ref. 3) involved atmospheric velocity of a meteoroid only to the negative second power. With use of that earlier factor, average velocities of meteoroids relative to Earth atmosphere have been estimated at values ranging from 20 (ref. 4) to 40 kilometers per second (ref. 5). The much greater negative exponent of atmospheric velocity in the weighting factor of reference 2 should be expected to cause a drastic reduction in estimated average velocity because it gives much greater weight to the counts of slower particles.

The magnitude and direction of the effect of the new weighting factor on estimates of influx rates of meteoroids of various masses, if any such effect exists, it is not immediately obvious. However, once the influx rate at various mass levels is determined, a calculation of average damage potential would obviously be affected strongly by the difference in effective average velocity arising from the difference between -2 and -4.22 as an exponent of atmospheric velocity in the weighting factor.

For this reason, an analysis was undertaken at the NASA Lewis Research Center to investigate the effect of the new weighting factor on estimated velocity distribution and on estimated influx rates at various mass levels for sporadic meteors. For this purpose, the Astrophysical Observatory of Smithsonian Institution provided valuable assistance in furnishing on punched cards observational data and various computed parameters for approximately 2400 photographic meteors. They were also very helpful in providing, in private communication, various items of further information about the photographic conditions. The data provided on punched cards were the same as published earlier by McCrosky and Posen (ref. 6).

Although the weighting factor must be applied to meteor velocity relative to Earth's atmosphere, the statistical results of the analysis were sought in terms of geocentric

velocities possessed by meteoroids before acceleration by Earth's gravity; that is, an overall influx rate and a distribution of influx rate relative to velocity were sought at a position in the Earth's orbit but far from Earth. Such results were desired, instead of real conditions near Earth, because (1) a description of the influx distributions should be mathematically simpler without the effect of Earth's gravitation and, hence, more readily susceptible of expression in the form of simple equations, (2) the influx distributions without the effect of Earth's gravitation would be encountered for long periods of time by a long-range space vehicle, and (3) on the basis of resulting equations representing the conditions before acceleration by Earth's gravity the conditions near Earth should be analytically derivable without need of further detailed statistical study.

The analysis was conducted in four stages. In the first stage, a computer program used the weighting factor and operated on the data for sporadic meteors of whatever mass to yield an adjusted velocity distribution. In the second stage, a similar computer program was used to obtain a velocity distribution for each of 10 intervals of mass, but without benefit of the weighting factor. In the third stage of the analysis, the result from stage 1 was compared with the result for the heaviest meteoroids from stage 2 to confirm or disprove an anticipated agreement. In stage 4 of the analysis, a distribution of meteoroid influx rates relative to mass was derived, with use of a method for correcting the count of meteors within each mass group for failures of observation due to insufficient brilliance of meteor trails.

INFLUX DISTRIBUTION RELATIVE TO VELOCITY

For the first stage of this analysis the theoretical basis will first be described, then the computer program will be explained briefly, and finally the resulting velocity distribution will be presented and discussed. Although most symbols are defined in appendix A, in general, each symbol will also be explained where first used.

Theory of Adjustment of Velocity Distribution

The weighting factor that was developed in reference 2 for use in determining adjusted velocity distributions is expressed by the equation

$$\varphi_w(1) = (\cos Z_R)^{-0.196} F\left(Z_R\right)_{av}^{0.730} v_\infty^{-4.22} \quad (1)$$

where Z_R is the angle between the meteoroid path and the zenith at the position of first encounter of the meteoroid with Earth atmosphere, v_∞ is the velocity of the meteoroid relative to Earth atmosphere at the same position, and $F(Z_R)_{av}$ is a statistical average function of Z_R and meteor position within the field of view of the cameras. The function $F(Z_R)_{av}$ was designed for the purpose of accounting for the random variation of position within field of view at which a meteor might appear. It was discussed in detail in reference 2 and, hence, will not be further explained here. For all meteors reported in reference 6, which formed the basis of the study to be reported here, values of $F(Z_R)_{av}$ were computed as part of the work reported in reference 2. The results remained available for use in the present study.

For study of velocity distributions of meteors as they encounter the atmosphere over New Mexico, the proper weighting of photographic meteors would be obtained by counting each meteor as one impact multiplied by the factor $\varphi_w(1)$ of equation (1). For the work reported herein, however, the factor was modified to include an adjustment for gravitational focussing, that is, the effect of Earth's gravitation in focussing the movement of particles in such a way as to increase the influx rate for all particles and to increase the influx rates for slower particles in comparison with faster ones. This additional adjustment was needed because, as explained earlier, it was desired to analyze the conditions existing before acceleration of meteoroids by Earth's gravity, rather than the actual conditions at Earth's surface.

The adjustment to compensate for the effect of gravitational focussing was taken from an equation developed by Shelton, Stern, and Hale (ref. 7). This equation and the manner of its use herein are discussed in appendix B. Its effect is to modify equation (1) to read

$$\varphi_w(2) = (\cos Z_R)^{-0.196} F(Z_R)_{av}^{0.730} v_\infty^{-4.22} \left[1 + \left(\frac{v_e}{v_G} \right)^2 \right]^{-1} \quad (2)$$

where v_e is the velocity of escape from Earth at the position where the meteor impacts the atmosphere and v_G is the unaccelerated velocity, which the particle would have had relative to Earth if Earth's gravity had not affected it.

Although $\varphi_w(2)$ as determined by equation (2) will provide adjustment of velocity distributions to the condition that would have obtained without the influence of Earth gravity, it still applies basically to the influx condition as it would then exist in the atmosphere over New Mexico, and predominantly during the later night-time hours. A statistically meaningful correction for the spacewise bias that exists would have required rejection of many meteors that were otherwise useable for statistical purposes because they came from logical subdivisions of the surrounding space that could not be com-

pletely sampled by the atmosphere over New Mexico during night-time hours. Such meteors, for example, arrive at the Earth atmosphere from directions south of the ecliptic or from directions relatively near that of the sun. It was believed the effect of the spacewise bias would not be great. For this reason and because of a belief that any attempt to correct the spacewise bias would unduly complicate this preliminary work, a decision was made to ignore the spacewise bias involved in the restriction of the exposure area to New Mexico during the later night-time hours.

A third weighting factor according to the equation

$$\varphi_{w(3)} = \left[1 + \left(\frac{v_e}{v_G} \right)^2 \right]^{-1} \quad (3)$$

was used for obtaining velocity distributions adjusted for gravitational focussing but not for the biasing effect of mass or the velocity v_∞ . For convenience in the following description of the general use of a computer program, a unity weighting factor is defined as

$$\varphi_{w(4)} = 1 \quad (4)$$

A computer program was written for the preparation of tabulations of values of v_G with use of the weighting factor $\varphi_{w(n)}$, with a value of 2, 3, or 4 for n . Data cards furnished by Smithsonian Institution Astrophysical Observatory were read and re-recorded for use with the computer program in a manner to ensure that the data for any pertinent meteor could not be overlooked on any run of the program. The cards contained exactly the data published in reference 6. They were checked with reference 6 for completeness. Data cards were excluded for meteors for which not all the needed data had been determined. In execution of the computer program, the following operations were performed for a single meteor, then for the next meteor, and so on.

(1) The parameters v_∞ , v_G , and $\cos Z_R$, were read, as well as serial number and the notation of shower association if present. (The parameters v_∞ , v_G , and $\cos Z_R$ correspond, respectively, to the column headings v_∞ , v_G , and CZ_R in table 7 of reference 6.) The value of $F(Z_R)_{av}$ as determined in the work reported in reference 2 was also read.

(2) The meteor was rejected from consideration if a shower association was indicated.

(3) The meteor was rejected from consideration if the value of $\cos Z_R$ was less than 0.20. (It was not believed this limitation would be statistically important; it resulted in rejection of approximately 20 meteors, or less than 1 percent of the total. This provision

was equivalent to limiting the acceptance of the atmosphere to a cone of approximately 102.5° included angle rather than 180° . The restriction was necessary because of the sensitivity of the weighting factor $\varphi_{w(1)}$ or $\varphi_{w(2)}$ to small errors in the smaller values of $\cos Z_R$. In particular, these factors go to infinity for $\cos Z_R = 0.00$. As several meteors were on the list with $\cos Z_R = 0.00$, they would have made use of these weighting factors quite impossible.)

(4) The value of $\varphi_{w(n)}$ was computed with a value of 11.1 kilometers per second for v_e (at an altitude of 90 km).

(5) The integer next higher than v_G in kilometers per second was found and the value of $\varphi_{w(n)}$ was added to the content of a storage location corresponding to that integer (initialized to zero at the start of the program).

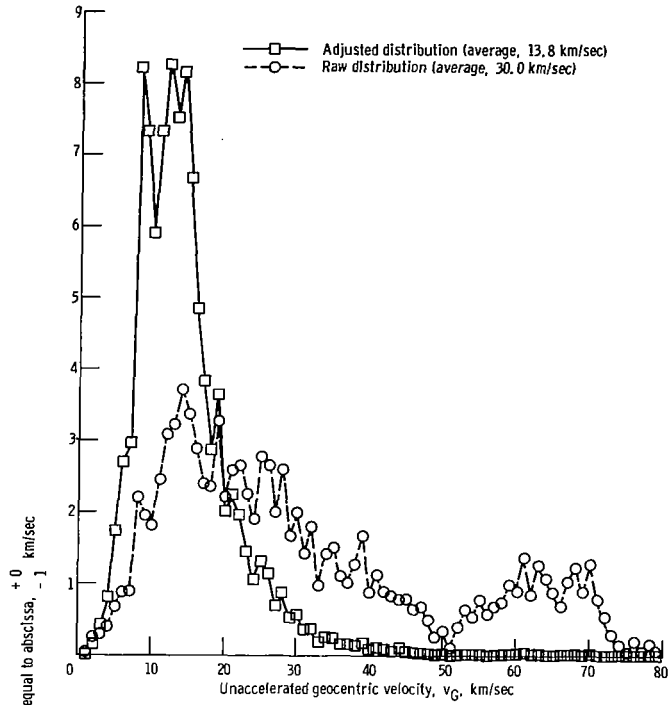
(6) The value of $\varphi_{w(n)}$ was multiplied by the value of v_G and added to the content of a storage location (initialized at zero) for later use in determination of average velocity.

After these operations had been performed for all meteors, the content of the storage location for each integral value of v_G was divided by the sum of the contents of all and multiplied by 100 to give the adjusted percentage of total count for each velocity interval. (Hereafter, this procedure for reduction of total counts to unity, or to 100 percent, will be referred to as "normalization." That term will also be used relative to the provision for unity, or 100 percent, area under a distribution curve. Factors or divisors used for the purpose will be referred to as normalizing factors or divisors.) The content of the storage location for use in determination of average velocity was also divided by the sum of the contents of all storage locations for integral values of v_G , to yield the average value of velocity.

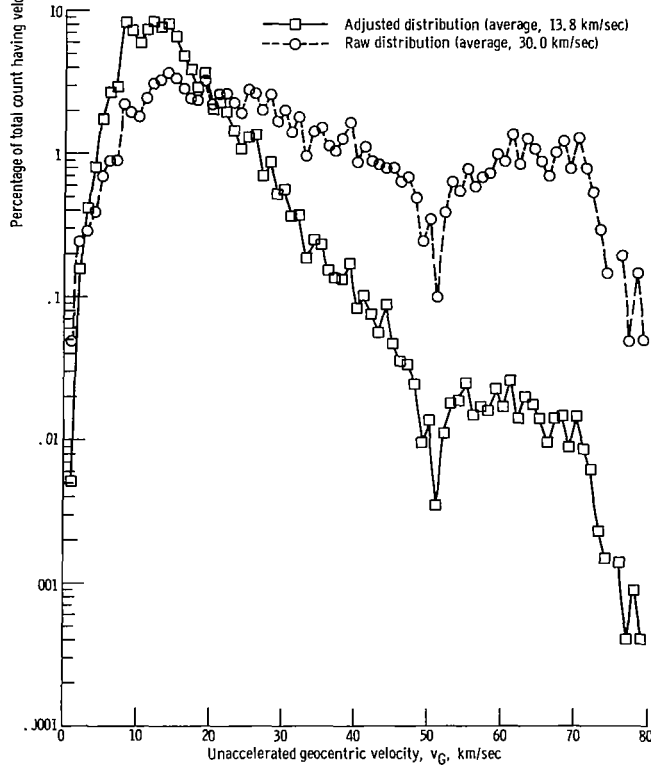
General Nature of Velocity Distribution

Results from runs of the program that has just been described, with n equal to 2 and with n equal to 4, are presented in figures 1 and 2 with several different plotting scales. These plots are actually histograms. However, for these figures and others, straight lines are drawn from one value to the next rather than the customary horizontal lines forming the tops of the bars. This change was made to avoid confusion in the comparison of two histograms in the same figure.

The raw distribution in the linear plot in figure 1(a) represents results obtained from the computer program with use of $\varphi_{w(4)}$ for each meteor, that is, with no adjustment even for gravitational focussing. It shows the familiar bimodal distribution with two peaks: one for direct orbits in the neighborhood of 14 kilometers per second, the other for retrograde orbits in the neighborhood of 60 to 70 kilometers per second. This



(a) Linear scale.



(b) Semilogarithmic scale.

Figure 1. - Comparison of raw distribution of velocity of meteors with distribution adjusted for photographic bias of meteoroid mass and velocity and for gravitational focussing.

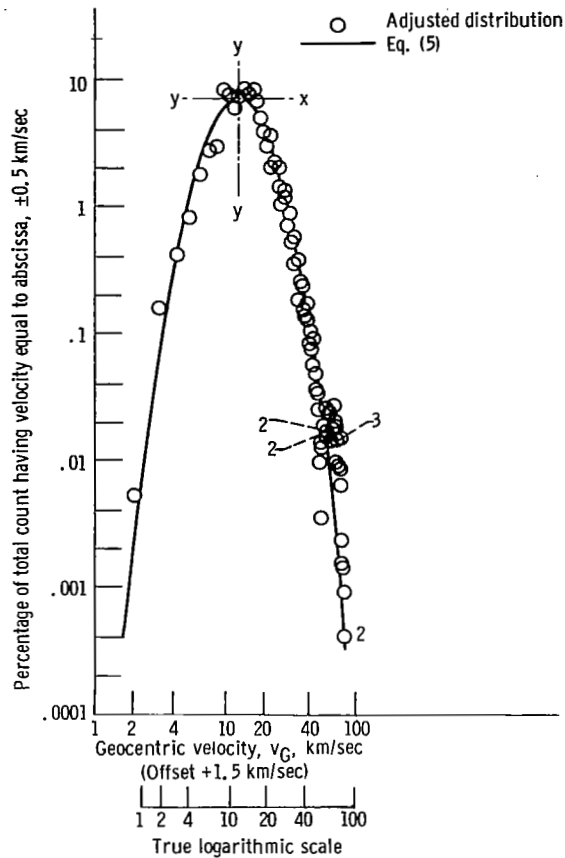


Figure 2. - Fit of log-normal equation to velocity distribution of meteors corrected for gravitational focussing and bias due to meteoroid mass and velocity.

distribution superficially indicates that particles in retrograde orbits might well represent the principal hazard because of their high velocities and substantial frequency.

However, the adjusted distribution in the same part of figure 1, obtained with use of $\varphi_w(2)$, shows that the retrograde orbits are comparatively rare and that the frequencies of velocities in the neighborhood of 8 to 18 kilometers per second are very high in comparison with all other velocities. The run of the program showed an average adjusted velocity (with $\varphi_w(2)$) of 13.8 kilometers per second as compared with a raw average (with $\varphi_w(4)$) of 30.0 kilometers per second.

The same results as plotted linearly in figure 1(a) are plotted on a similogarithmic scale in figure 1(b). Here, it is seen that the peak of the adjusted distribution for retrograde orbits is lower by more than two orders of magnitude than the peak for the

direct orbits. Although the adjusted distribution is still bimodal, the departure from a single mode is not nearly so great as in the raw distribution. It is seen that both raw and adjusted curves drop to very low levels in the neighborhood of 1 to 2 kilometers per second. Such particles would have to have orbits almost the same as that of the Earth and nearly the same velocity relative to the sun. It will be seen that, below 3 kilometers per second, the adjusted distribution falls under the raw distribution. This condition exists because, in this velocity range, the adjustment for gravitational focussing that is included within the function $\phi_w(2)$ exceeds the adjustment for effect of mass and velocity on luminosity.

The same results for adjusted velocity distribution as shown in figure 1 are plotted in figure 2 on a full logarithmic scale. The values shown on the abscissa scale are true values of the midpoints of the 1-kilometer-per-second velocity intervals shown on the abscissa scales in figure 1. However, they are shifted 1.5 kilometers per second toward the right relative to the logarithmic scale. This shift resulted from a trial-and-error procedure to obtain the best possible fit of a curve representing a distribution equation to the plotted points. The results, as delivered by the computer and as plotted in figure 1, were referred to the maximum of each velocity interval. Hence, the offset of points by 1.5 kilometer per second (fig. 2) is an offset of only 1 kilometer per second relative to the abscissa scales of figure 1. In cases where two or more data points were too close together to plot separately in figure 2, a single point was plotted and the numeral 2 or 3 was entered in the figure to indicate that such a number of data points correspond to the plotted position.

The curve in figure 2, which appears to represent the plotted results closely, is a true parabola. As shown in appendix C, it represents the following offset log-normal equation.

$$f(v_G) = 0.07 \exp \left\{ -\frac{1}{2} \left[\frac{\log_e (v_G + 1.5) - \log_e 11.7}{0.44} \right]^2 \right\} \quad (5)$$

So it is seen that equation (5), plotted as the parabola in figure 2, represents a tentative analytical velocity distribution that closely describes the data. No theoretical reason is offered as to why the distribution should be log-normal with an offset of 1.5 kilometer per second; the discovery is empirical.

For geocentric velocities below 30 kilometers per second, equation (5) represents very roughly the same normal distribution as reported by Wall (ref. 9), which he derived by other methods. At higher velocities, the distribution according to equation (5) differs greatly from his.

RAW VELOCITY DISTRIBUTIONS FOR MASS GROUPS

In the second stage of the analysis, unaccelerated velocity distributions (histograms) were obtained for each of 10 mass groups with use of weighting factor $\phi_{w(3)}$. These histograms will be used for comparisons with the histogram for all sporadic meteors, adjusted with weighting factor $\phi_{w(2)}$, by which the most essential objectives of this analysis will be accomplished. Hereinafter, the distributions for the 10 mass groups, with adjustment only for gravitational focussing, will be referred to for brevity as "velocity distribution for mass group 1," "velocity distribution for mass group 2," and so on, or collectively "velocity distributions for mass groups." The distribution earlier described, obtained for sporadic meteors of all masses with use of weighting factor $\phi_{w(2)}$ (plotted as the square symbols in fig. 1 and as the round symbols in fig. 2), will be referred to hereinafter as the "velocity distribution for all masses."

To obtain the velocity distributions for mass groups, the data cards for all photographed meteors were sorted to eliminate cards for which mass was not given and to arrange the remaining cards in order of descending mass. The cards were then physically divided into 10 mass groups, each containing the same number of cards $\pm 1/2$ card. The computer program earlier described was used to tabulate the distribution of velocity v_G for each of the 10 mass groups with use of weighting factor $\phi_{w(3)}$, excluding each shower-associated meteor as before. The percentage of shower-associated meteors proved to be substantially higher for low masses than high, so that the meteors left in each mass group after rejection of the shower-associated meteors ranged from 217 in the heaviest group to 172 in the lightest. However, the lighter groups were still thought to be large enough to be statistically significant. The groups were used without change, in preference to redividing them with a consequent extension of the higher mass ranges downward into the lower masses.

The velocity distribution for each of the 10 mass groups resulting from the computer tabulations is plotted in figure 3. Also plotted in figure 3 is the velocity distribution for all masses.

The velocity distributions for the 10 mass groups are normalized with implicit use of a divisor believed to be equal to the true total influx rates for those groups, which in most cases differed from the observed influx rates. The manner of this normalization

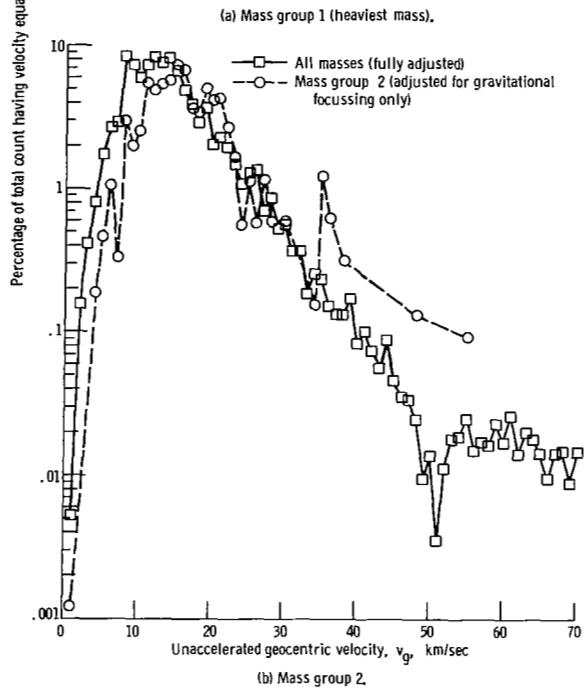
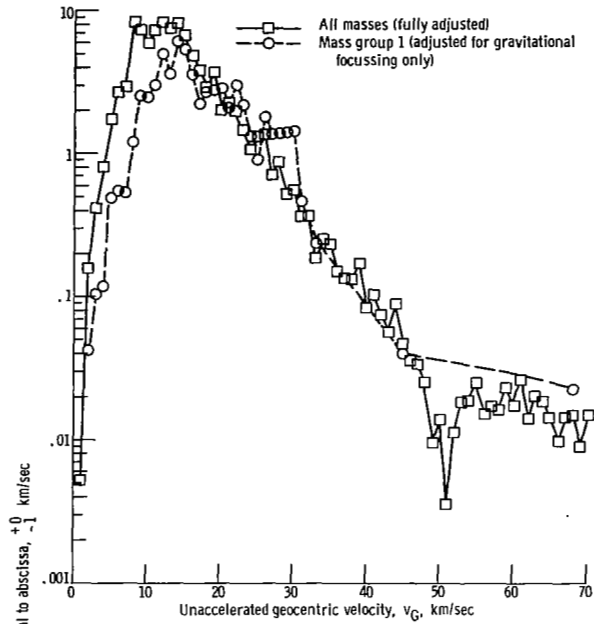
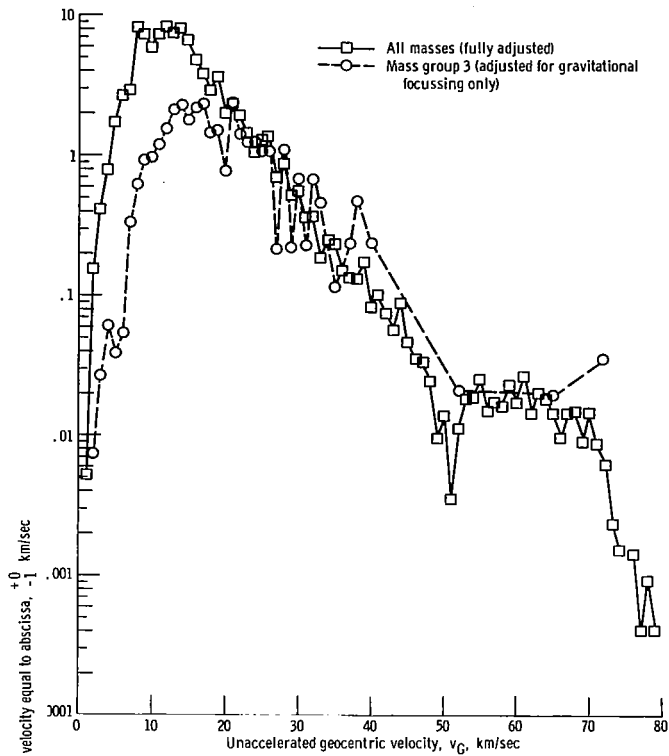
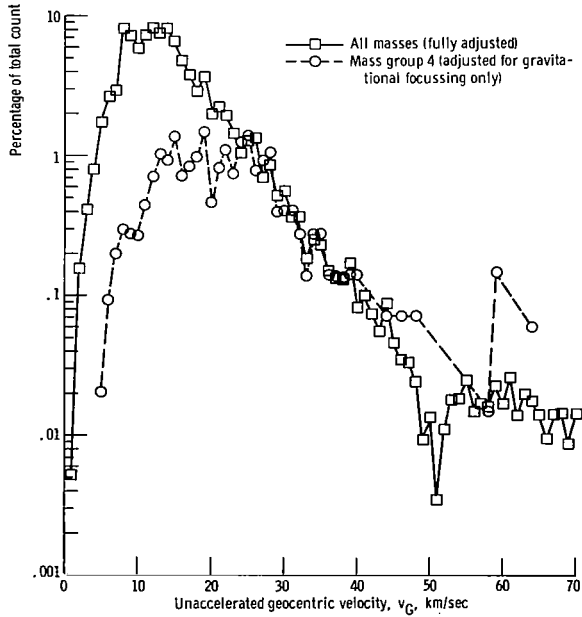


Figure 3. - Comparison of distributions of velocity of meteors within specific mass groups with distribution for all masses adjusted for photographic bias of meteoroid mass and velocity.

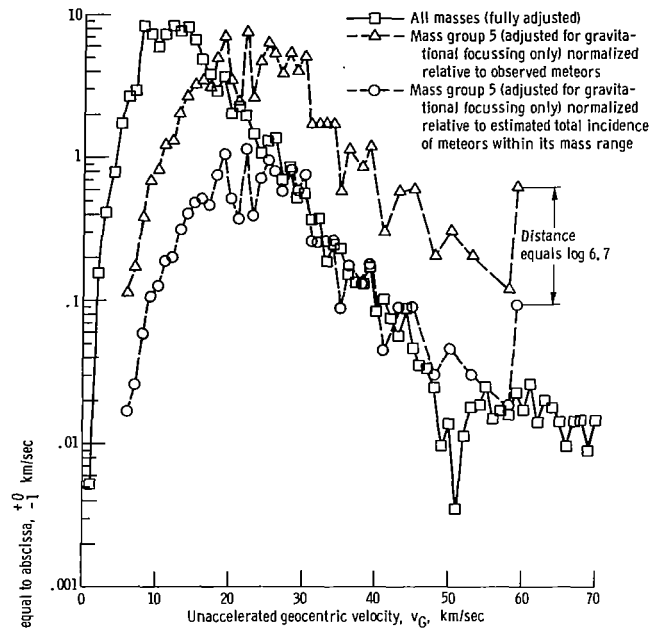


(c) Mass group 3.

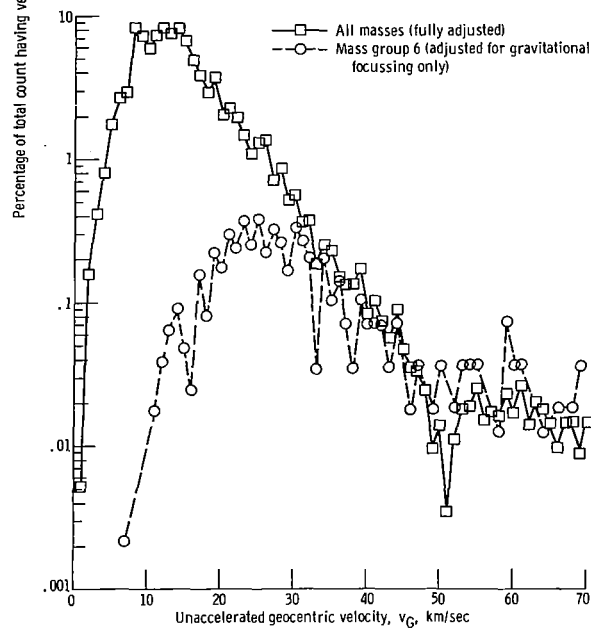


(d) Mass group 4.

Figure 3. - Continued.



(e) Mass group 5.



(f) Mass group 6.

Figure 3. - Continued.

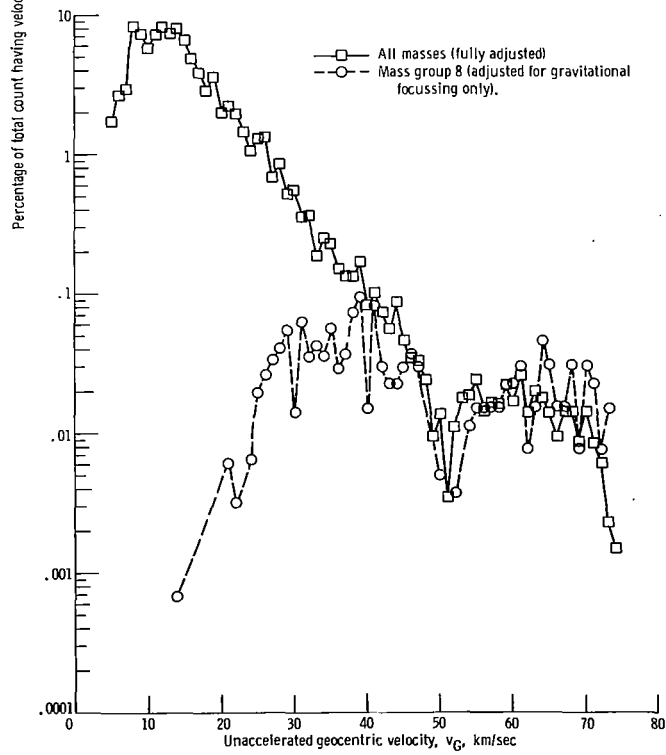
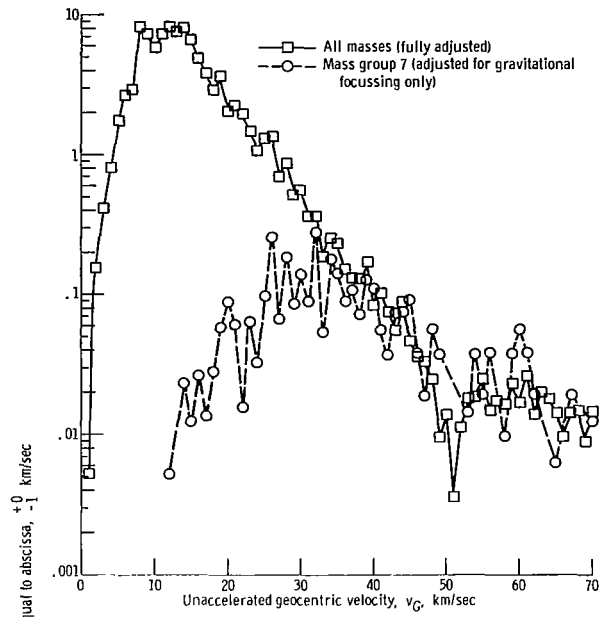
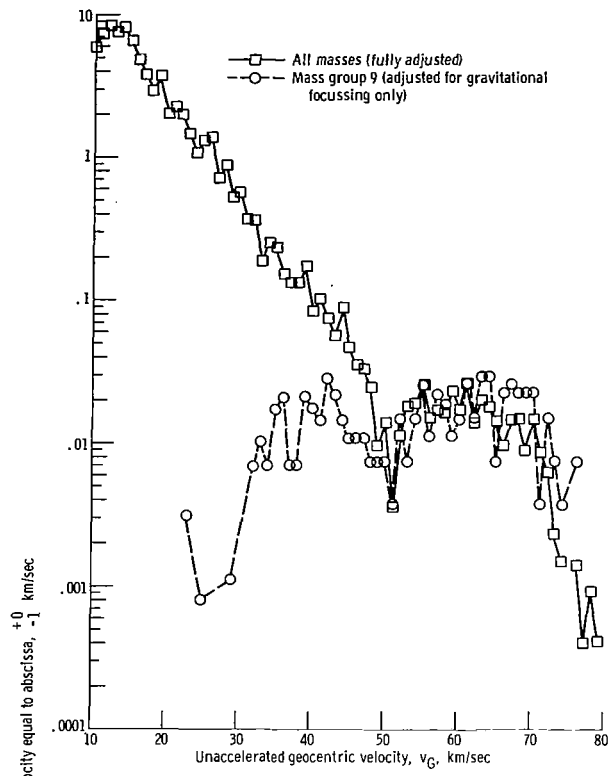
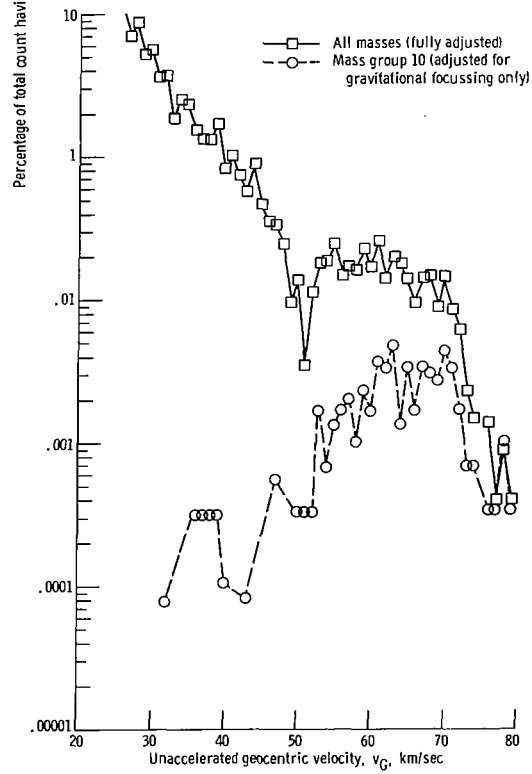


Figure 3. - Continued.



(i) Mass group 9.



(j) Mass group 10.

Figure 3. - Concluded.

will be described somewhat later. In the single case of mass group 5 (fig. 3(e)), the distribution for the group is also shown normalized by using a divisor equal to the observed influx rate corrected only for the effect of gravitational focussing. The additional plotting is shown in this part of figure 3 because it was chosen as the most convenient figure for later detailed discussion.

The velocity distributions for the mass groups in general cannot be regarded as realistic, because they have no correction for the velocity bias that existed in the photographic process. Their only purpose is for use in the following analytical comparisons.

RAW VELOCITY DISTRIBUTION FOR HEAVIEST METEORIODS

The third stage of the analysis involves investigation of the prediction that an adjusted velocity distribution should not differ from an unadjusted distribution for a very heavy mass group whose lower limit of mass will be termed m_{\min} . In reference 2, in the development of the expression for $\phi_w(1)$, an assumption was used to the effect that the velocity distribution is substantially the same for any mass within the photographic range. Such assumption appears to be reasonable (1) because the mass of a particle does not enter into the equations that interrelate orbital parameters (including velocity) and (2) because no theoretical mechanism is known to produce substantial orbital changes on a mass basis within the mass range involved in this study, except possibly at very low geocentric velocities (circular orbits) where the Poynting-Robertson effect (ref. 10) might assume some importance.

If the assumption of the same velocity distribution for any mass is correct and if equation (1) is also correct, it should be expected that the velocity distribution for all masses, determined with use of weighting factor $\phi_w(2)$, might be identical with a velocity distribution for a very heavy mass group, obtained with use of weighting factor $\phi_w(3)$. For, if the value m_{\min} within the group were great enough, virtually all meteoroids within the group should produce trails that could be easily photographed regardless of velocity. The minimum practical limit of velocity of impact on the atmosphere should be the velocity of escape from Earth. Hence, if the value of m_{\min} were great enough to allow easy photography at the velocity of escape, few meteoroids at any impact velocity would escape detection.

Striking confirmation of the prediction described is shown in a comparison of results presented in figure 4. The dashed-line histogram in that figure represents the average distribution of velocities v_G for the two heaviest mass groups, normalized relative to the observed count of meteors adjusted with use of weighting factor $\phi_w(3)$. Initially, the decision was made to use the total content of the first two mass groups for the comparison in this figure because the histograms for these two groups looked very much alike.

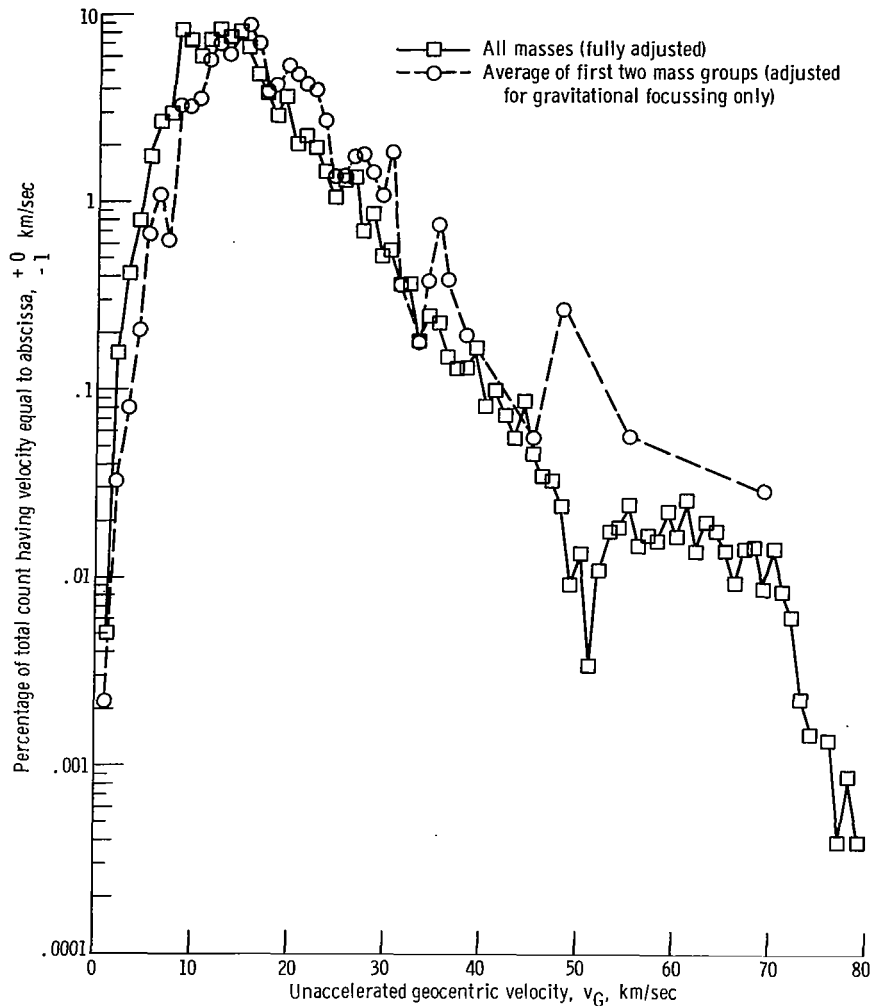


Figure 4. - Comparison of distribution of velocity of meteors within combination of two heaviest mass groups with distribution for all masses adjusted for photographic bias due to meteoroid mass and velocity. (Both plots are adjusted for effect of gravitational focussing).

A more elaborate indication that this choice was a good one will be mentioned later. The solid-line histogram in figure 4 is the velocity distribution for all masses, as earlier defined and as sketched earlier in figure 1(b).

Throughout the velocity range from about 20 to 79 kilometers per second, the two histograms show the same general trend, but with the histogram for the two heaviest mass groups generally on a slightly higher level. In the velocity range from 1 to about 10 kilometers per second the trends are again similar, but with the relative levels reversed. The differences of level are slight, and the comparison, therefore, amounts to

a general confirmation of the validity of the adjusting factor $\phi_{w(1)}$. Specifically, the appearance of the two histograms in figure 4 for geocentric velocities above 20 kilometers per second is a confirmation, as exact as the point-to-point irregularities permit, of the assumption used in reference 2 that the same velocity distribution exists for all masses.

Two possible causes of the failure of the adjusting factor $\phi_{w(2)}$ to provide exact agreement between the two histograms will be discussed.

(1) Some failure to observe low-velocity meteors because of faintness of the traces in the photographic plates may have occurred even within the heaviest mass groups. If the meteor sample had been larger, the heaviest groups could have been further subdivided to determine whether the raw histograms for the heaviest subdivision might have duplicated the adjusted histogram for all masses. But such subdivisions would not have provided a large enough sample within each subdivision to serve as an adequate statistical base. One slight indication contrary to this explanation is the close agreement between the raw histograms for mass groups 1 and 2 in figures 3(a) and (b).

(2) In the derivation of the factor $\phi_{w(1)}$ in reference 2, it was not possible to take into account the effect of meteoroid fragmentation. As discussed in that reference, fragmentation should tend to increase the brilliance of a meteor. Fragmentation is also known generally to cause a more pronounced effect with meteors of lower speed (refs. 11 and 12). The factors $\phi_{w(1)}$ and $\phi_{w(2)}$ were designed to magnify real counts of meteors in a manner dependent, among other things, on their faintness. If, due to fragmentation, the meteors of lower speeds are not actually as faint as they were treated in the derivation of the factor $\phi_{w(1)}$, then that factor would excessively magnify the count of meteors in the low-speed range and cause the slight systematic discrepancy between the two histograms that is seen in figure 4.

The question of disagreement of these histograms in the low-velocity region can not be resolved here, but must await later study. The assumption of a single velocity distribution for all masses and the correctness of the weighting factor $\phi_{w(1)}$ for velocities lower than about 20 kilometers per second are only approximately confirmed. But they are not contradicted by the appearance of the histograms, even on an exact basis.

Hereinafter explanation (2) for this anomaly will be treated as the correct explanation, but with the reservation that later research may show explanation (1) to be correct. No significant change in final results would then be required.

INFLUX DISTRIBUTION RELATIVE TO MASS

Determination of an influx distribution relative to mass will now be undertaken as the last stage of this analysis. Hereinafter, that influx distribution will be called "mass distribution."

Meteoroid Mass Determination

In determination of a mass distribution from the data of reference 6, some uncertainty exists concerning a basic reference level. The reference level used here places the upper and lower limits of the 10 mass groups at values that do not relate directly to the masses given in reference 6. They have been adjusted upward from the values of reference 6 by a factor 6.4.

Since the publication of reference 6, the most probable value of luminosity coefficient of meteors has been revised. As stated in that reference, meteoroid mass m was determined by integration of the equation

$$m = \frac{2}{\tau_0 v^3} \int_0^T I dt \quad (6)$$

where τ_0 is the luminosity coefficient used in reference 6, v is the instantaneous velocity, T is the lifetime of the meteor, and I is the instantaneous luminous intensity. It is apparent, therefore, that a corrected mass m_{cor} should be expressed as

$$m_{\text{cor}} = m \frac{\tau_0}{\tau_{0(\text{cor})}} \quad (7)$$

where $\tau_{0(\text{cor})}$ is the value of luminosity coefficient considered to be most probable at this time.

From information given in references 6 and 13 to 15, a value

$$\frac{\tau_0}{\tau_{0(\text{cor})}} = 6.4 \quad (8)$$

was deduced for use in equation (7) for the purposes of the present analysis. After completion of the analysis, but before publication, reference 16 became available. On page 4 of that reference there is indication that the ratio should be

$$\frac{\tau_0}{\tau_{0(\text{cor})}} = 6.46 \quad (9)$$

As equations (8) and (9) are nearly identical, further justification of the factor 6.4 used in the present analysis will not be included herein.

Correction of Counts of Meteors

A method was found for correction of the counts of meteors within the 10 mass groups for failure of observation. The method involves a comparison between the velocity distribution for all masses as earlier defined (the solid-line histogram of figs. 1(b) and 4) and each of the 10 dashed-line histograms (fig. 3). Those 10 histograms, as explained earlier, represent the unaccelerated velocity distribution for each of the 10 mass groups, adjusted only for gravitational focussing.

In the comparison a choice was necessary, whether to use the solid-line histogram of figures 1(b) and 4 or the dashed-line histogram of figure 4. The decision was made to use the histogram first mentioned because (1) only the parts of the histogram above about 20 kilometers per second will have importance in the comparisons and (2) in all velocity regions above about 20 kilometers per second, the histogram used for comparison needs to be as accurate as possible. The dashed-line histogram in figure 4 is not dependable above about 35 kilometers per second. Above the geocentric velocity of 35 kilometers per second, in the two groups of greatest mass, meteors were found only at velocities of 36, 38, 45, 48, 55, and 69 kilometers per second. A solution of the problem of plotting the percentages of total influx at these isolated velocities in such a manner that the values would be significant in relation to the other parts of the histogram involves unavoidable compromise and uncertainty. (This problem also exists at both high and low velocities for the dashed-line histograms of the various parts of figure 3.) The problem was resolved in an arbitrary and not entirely satisfying manner by assuming, after normalization, that an isolated count should be distributed impartially between the velocity class within which it actually occurred and the velocity classes separating it from the nearest nonvacant class in the direction toward the main body of the data. A point was actually plotted, however, only for the velocity class within which the count occurred.

The count of meteors within a mass group, before correction, was the total count for all velocity classes delivered by the computer program with use of the weighting factor $\varphi_w(3)$. This factor provided an adjustment only for gravitational focussing, by counting each sporadic meteor as one multiplied by the factor $\varphi_w(3)$. The first step in the use of the counts for the mass groups was the determination of a basic factor α^1 by which the counts for the various masses could be multiplied to convert them to particles per square meter per second. For this purpose all meteors of any mass of magnitude equal to or less than zero were counted, without adjustment even for effect of gravitational focussing. The resulting total count (436) was used in conjunction with

equation (16) of reference 17 which reads as follows:

$$\log_{10} N_0 = -4.33 \quad (10)$$

where N_0 is frequency of occurrence of meteors of magnitude zero or brighter per square kilometer per hour. Such equation was accepted as correct for the purpose of this analysis. On such basis, a value of α' by which any count may be multiplied to convert it to particles per square meter per second is

$$\alpha' = \frac{(4.68 \times 10^{-5}) \times 10^{-6}}{436 \times 3600} = 2.982 \times 10^{-7} \quad (11)$$

that is,

$$C = C' \alpha' \quad (12)$$

where C' is a count of meteors of a given mass range adjusted for gravity focussing or not and C is a corresponding frequency of influx in particles per square meter per second.

As mentioned earlier, no adjustment for spacewise bias in the photography was made for the present analysis. It appears, also, that no adjustment for the spacewise bias was made in the work of reference 17. Hence, equation (11) will be applicable to the atmosphere over New Mexico during the late night-time hours rather than to a randomly oriented surface in space. The equation will therefore be in harmony with the velocity distributions and the counts of meteors of various masses as they will be used in the present analysis.

In the description of the next steps in the procedure, involving adjustment of the counts, the fifth mass group will be used as an illustrative example. It was chosen for discussion because the features to be studied are more clear cut than in other cases. However, exactly the same procedure as that which will be described relative to mass group 5 was used for each of the mass groups in turn. For each mass group i , the computer count of meteors adjusted with weighting factor $\phi_w(3)$ will be designated $C_{a(i)}$.

The solid-line histogram in figure 3(e) shows the velocity distribution for all masses. It is the same as the solid-line histogram of figure 1(b) or figure 4.

The shape of the velocity distribution for mass group 5, with adjustment for gravity focussing, appears as two dashed-line histograms in figure 3(e), on levels corresponding to the use of two different normalizing divisors as earlier described. These two differently normalized histograms will be discussed in more detail.

Before the construction of figure 3(e) the normalizing divisor for the triangular points (132.4) was known, simply as the computer's count of meteors adjusted only for gravitational focussing. The normalizing factor for the circular points was determined by the construction of the figure which involved the implicit use, mentioned earlier, of a normalizing factor believed equal to the true influx for the mass group.

If the histogram for all masses (the square points) is actually correct as the velocity distribution for the fifth mass group, then it should agree with the histogram for mass group 5 as to shape on the semilogarithmic plot everywhere to the right of some critical geocentric velocity. That critical geocentric velocity should be the velocity at which even the particle of smallest mass within the group would be bright enough to be discovered without failure on the photographic plates. At lower velocities, at least occasional failure would occur in the discovery of meteors even though they might have great enough mass to place them within the group. At those lower velocities, the failure to discover faint meteors would cause the histogram for mass group 5 to be on too low a level in comparison with the higher velocities. The histogram would therefore not have the same shape as the solid-line histogram at these lower velocities.

In consequence, the correct level for the histogram representing the velocity distribution for mass group 5 may be found simply by moving the histogram downward without change of shape from the original position represented by the triangular symbols to the position shown by the circular symbols. The correct level should be reached when the maximum agreement exists between the solid-line histogram and the dashed-line histogram within the parts of those histograms generally toward the right. Such a maximum agreement was thought to exist when the dashed-line histogram reached the level shown by the circular symbols, on a lower level than that shown by the triangular symbols by a distance equal to $\log 6.70$.

At the lower level, the velocity distribution for all masses (square points) coincides with that for mass group 5 (circular points), in general level and in shape, as exactly as could be desired throughout the velocity range from about 28 to about 58 kilometers per second. Below that velocity range, the histogram for mass group 5 falls off below that for all masses because of the marginal luminosity for particles in this mass group at these lower velocities. On the other hand, at velocities above about 39 kilometers per second the population density of this mass group was so small (10 meteors total) that great weight could not have been given to the level of the dashed-line histogram within that velocity range, even if it had not agreed well with the solid-line histogram.

From inspection of figure 3(e) the critical velocity above which the histograms agree, for the fifth group, is about 28 kilometers per second. As demonstrated in appendix D, the distance of the downward shift of the dashed-line histogram necessary to bring about agreement of the two histograms throughout the velocity region above the critical should be the logarithm of a correcting factor ϕ by which the count of particles in the mass

group should be multiplied to make that count correct; that is, with substitution of $\varphi'_{(i)}$ for φ of appendix D, for mass group i ,

$$C'_i = C_{a(i)} \alpha' \varphi'_{(i)} \text{ particles m}^{-2} \text{ sec}^{-1} \quad (13)$$

where C'_i is an influx rate for mass group i corrected for the shift of the histogram. The amount of the necessary shift in the case of mass group 5 was measured as

$$\log \varphi'_{(5)} = \log 6.70 \quad (14)$$

while the value of $C_{a(5)}$ delivered by the computer was 132.4 meteors. Consequently, by equation (13) the count for mass group 5 corrected for the shift of the histogram should be

$$C'_5 = 132.4 \alpha' \varphi'_{(5)} = 2.65 \times 10^{-14} \text{ particles m}^{-2} \text{ sec}^{-1} \quad (15)$$

All other parts of figure 3 show the same solid-line histogram as in figures 1(b), 4, and 3(e). Also, each part of figure 3 shows a dashed-line histogram for one of the mass groups from 1 to 10. In each case, as has been explained in reference to figure 3(e), the dashed-line histogram has been shifted downward by the necessary amount to bring it into agreement with the solid-line histogram throughout the velocity range above which particles are not lost because of faintness of exposure. In the downward shifting of the dashed-line histograms, little weight was given to the highest velocity regions if the population density in such regions was sparse. In each case, as with figure 3(e), the distance of the downward shift is the logarithm of a correcting factor $\varphi'_{(i)}$ for application to the observed count $C_{a(i)}$, for use in equation (13).

Values of $\log \varphi'_{(i)}$ obtained by the method described for the 10 mass groups are tabulated in table I. Also shown is the lower limit of mass for each group.

The count C'_5 of equation (15) and analogous counts C'_i for other mass groups, corrected for the shifts of the histograms, need an additional correction. From figure 4 an inference may be drawn that the velocity distribution for all masses is on too low a level throughout the velocity range above about 20 kilometers per second, because it appears to be on too high a level at lower velocities. Figure 4 should not be interpreted as an indication that meteoroids of geocentric velocity less than 10 kilometers per second are more rare for greater masses than for lower masses. The meteors of these lower velocities that were actually observed were all of large mass. A greater actual count at these lower velocities would have raised the level of both histograms in figure 4 proportionately, and a lower actual count would have lowered both proportionately. So instead, as discussed earlier, the condition under discussion will be treated

TABLE I. - HISTOGRAM SHIFTS FOR
VARIOUS MASS GROUPS

Mass group	Shift required to cause histograms to superimpose in regions of higher velocity, $\text{Log } \varphi'_{(i)}$	Lower mass limit, g	Figure
1	$\log (1.54)$	0.705	3(a)
2	$\log (1.25)$.397	3(b)
3	$\log (2.90)$.250	3(c)
4	$\log (4.45)$.1603	3(d)
5	$\log (6.70)$.1025	3(e)
6	$\log (17.0)$.0641	3(f)
7	$\log (29.0)$.03786	3(g)
8	$\log (72.0)$.01922	3(h)
9	$\log (150.0)$.0077	3(i)
10	$\log (1700)$.000635	3(j)

as an indication that because of the effect of fragmentation factor $\varphi_{w(1)}$ or $\varphi_{w(2)}$ is not quite correct, at least for comparison of the velocity region below about 10 kilometers per second with that above about 20 kilometers per second. The apparent inaccuracy causes the adjusted velocity distribution for all masses to show too high an influx rate at velocities less than about 10 kilometers per second. Conversely, then, the indicated influx rate at velocities higher than about 20 kilometers per second must be too low. The effect of this incorrect level on the counts of meteors should now be considered.

In the preceding parts of the analysis, the incorrect shape of the histogram for all masses within the velocity range below 20 kilometers per second has been of no consequence. For, on examination of appendix D, it may be seen that the entire correct histogram for all masses is not needed. The derivation is equally valid if it is assumed that only the portion being matched has the correct shape and level. However, because of the incorrect level of the utilized part of the histogram for all masses, all the shifts of dashed-line histograms that were made in construction of figure 3 were actually greater than they should have been by a constant amount. That amount may be estimated from the values of $\log \varphi'_{(i)}$ tabulated in table I as follows.

It is observed that the values of $\log \varphi'_{(1)}$ and $\log \varphi'_{(2)}$, namely, $\log (1.54)$ and $\log (1.25)$, progress in the opposite sense to the progression from $\log \varphi'_{(2)}$ through $\log \varphi'_{(10)}$. The comparison of $\log \varphi'_{(1)}$ and $\log \varphi'_{(2)}$ would seem to indicate a need for a greater adjustment for meteors too faint to photograph in mass group 1 than in mass group 2. This condition cannot logically exist. For that reason, mass groups 1 and 2, and only they, are believed to include only masses so great that the meteoroids practically never escape detection however low their geocentric velocities. (This condition is

the earlier mentioned independent confirmation that the total content of mass groups 1 and 2 was a good choice for use in the comparison that was made in fig. 4.) Accordingly, $\log \varphi'_{(1)}$ and $\log \varphi'_{(2)}$ should be equal. The difference between them must be due to random irregularities or inexactness of the method. Moreover, if the histogram for all masses were correct at geocentric velocities above about 20 kilometers per second, both $\varphi'_{(1)}$ and $\varphi'_{(2)}$ should equal zero. Hence, the average of these two values should be at least a fair measure of the excess shift of the dashed-line histograms, not only for groups 1 and 2 but for all 10 mass groups. Accordingly, a corrected shift, $\varphi_{(1)}$, is defined by the equation

$$\log \varphi_{(i)} = \log \varphi'_{(i)} - \frac{\log(1.54) + \log(1.25)}{2} \quad (16)$$

or

$$\log \varphi_{(i)} = \log \varphi'_{(i)} - \log(1.39) \quad (17)$$

For any mass group i , the shift $\varphi'_{(i)}$ together with equation (17) permits the writing of an expression for a fully corrected count of meteors for the group as

$$C_i = C_{a(i)} \alpha^i \varphi_{(i)} \quad (18)$$

Thus, in the final result, equation (18) replaces equation (13), C_i replaces C'_i of equations (13) and (15), and $\varphi_{(i)}$ replaces $\varphi'_{(i)}$ in equations (13) to (15). In particular, for mass group 5, equation (15) is changed to

$$\begin{aligned} C_5 &= C_{a(5)} \alpha^5 \varphi_{(5)} = 132.4 \times 2.982 \times 10^{-17} \times \frac{6.70}{1.39} \\ &= 1.902 \times 10^{-14} \text{ particles m}^{-2} \text{ sec}^{-1} \end{aligned} \quad (19)$$

As mass group 1 contains all meteors of mass greater than its lower limit, a fully corrected cumulative count for any mass group i may be determined with use of equation (18) as

$$C_{\text{cum}(i)} = \sum_{j=1}^{j=i} C_j \quad (20)$$

or

$$C_{\text{cum}(i)} = C_{\text{cum}(i-1)} + C_i \quad (21)$$

As the same procedure that has been described with mass group 5 as an example was used with each mass group 1 to 10 in turn, a value of $C_{\text{cum}(i)}$ was determined with use of equation (20) for $i = 1$ and with use of equation (21) thereafter. For mass group 4 the result was

$$C_{\text{cum}(4)} = 2.916 \times 10^{-14} \text{ particles m}^{-2} \text{ sec}^{-1} \quad (22)$$

Accordingly, for the fifth mass group, from equations (19), (21), and (22)

$$C_{\text{cum}(5)} = C_{\text{cum}(4)} + C_5 = 4.818 \times 10^{-14} \text{ particles m}^{-2} \text{ sec}^{-1} \quad (23)$$

RESULTS

Tabulated in table II, for each of the 10 mass groups, are value of count of meteors $C_{a(i)}$ corrected only for the effect of gravitational focussing, logarithmic correction

TABLE II. - UNACCELERATED METEOROID INFLUX DISTRIBUTION RELATIVE TO MASS

Mass group	Count corrected for gravity focussing, $C_{a(i)}$	Log of correction factor for unobserved faint meteors, $\log \varphi(i)$	Fully corrected count, C_i , particles $\text{m}^{-2} \text{sec}^{-1}$	Fully corrected cumulative count, $C_{\text{cum}(i)}$, particles $\text{m}^{-2} \text{sec}^{-1}$	Lower mass limit, g	Figure
1	132.1	$\log(1.11)$	3.94×10^{-15}	3.94×10^{-15}	0.705	3(a)
2	109.8	$\log(0.90)$	3.28×10^{-15}	7.22×10^{-15}	.397	3(b)
3	129.6	$\log(2.08)$	8.06×10^{-15}	1.528×10^{-14}	.250	3(c)
4	145.5	$\log(3.20)$	1.388×10^{-14}	2.916×10^{-14}	.1603	3(d)
5	132.4	$\log(4.82)$	1.902×10^{-14}	4.818×10^{-14}	.1025	3(e)
6	133.2	$\log(12.22)$	4.86×10^{-14}	9.68×10^{-14}	.0641	3(f)
7	152.6	$\log(20.85)$	9.48×10^{-14}	1.916×10^{-13}	.03786	3(g)
8	139.2	$\log(51.8)$	2.15×10^{-13}	4.07×10^{-13}	.01922	3(h)
9	132.8	$\log(108.0)$	4.28×10^{-13}	8.35×10^{-13}	.0077	3(i)
10	119.7	$\log(1223)$	4.36×10^{-12}	5.20×10^{-12}	.000635	3(j)

factor $\varphi_{(i)}$ according to equation (17), fully corrected count C_i according to equation (18), fully corrected cumulative count $C_{cum(i)}$ according to equation (20) or (21), and lower mass limit. In the computation of fully corrected counts C_i as shown in table I, two minor departures were made from the procedure that has been described. For mass group 1, the excess value of $\varphi_{(1)}$ above unity is contrary to the earlier conclusion that no particles in mass group 1 could have escaped detection because of low velocity. The excess was considered to be due to inaccuracy of the method and the value was treated as exactly unity. For mass group 2, the deficit of $\varphi_{(2)}$ below unity would correspond to a negative number of particles escaping detection because of low velocity. Hence, the deficit was considered to be due to inaccuracy of the method and the value was treated as exactly unity.

The values of fully corrected cumulative count $C_{cum(i)}$ as shown in table II are plotted on a full logarithmic scale relative to the group lower limits of particle mass as the circular points in figure 5. The straight line in the figure representing the results of the present analysis was constructed on the basis of the points for mass groups 1 to 8. It virtually passes through each of these points. The plotted points for mass groups 9 and 10 were given no weight in the construction of the line because it was fully expected that these points would fall below their correct levels. From examination of figure 3 it is clear that the photographic exposure threshold is not sharply defined; that is, instead of a sharp cut off below a particular velocity for a given mass, there is a gradual failure to detect particles of progressively lower velocity. It follows reasonably that, if all particles of mass equal to or greater than the minimum of the 10th mass group had been

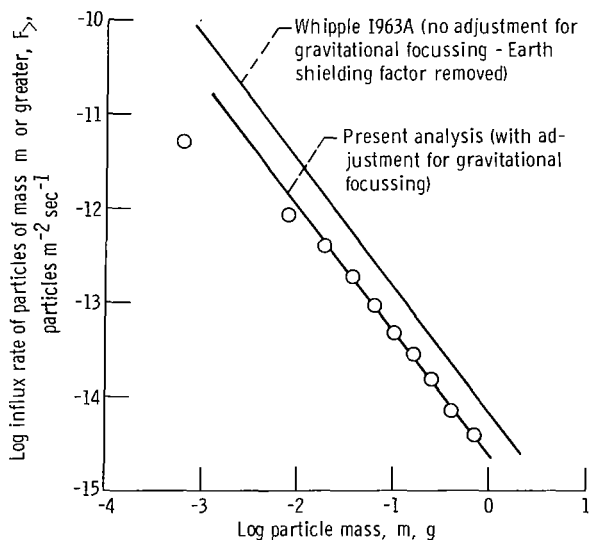


Figure 5. - Distribution of influx rate of meteors relative to mass.

detected, even at the highest velocities of 77 to 79 kilometers per second, then some particles of even smaller mass would have been detected at those velocities. As none such were detected, it follows that particles with mass that would have placed them in the 10th group and velocities in the neighborhood of 77 to 79 kilometers per second must have gone undetected. In comparing the two histograms of figure 3(j), nothing better could be done than to place the points of the two histograms level at velocities of 77, 78, and 79 kilometers per second. Undoubtedly, the points for mass group 10 should have gone lower even in that velocity range. Hence, in view of the demonstrated absence of a sharp cutoff at the exposure threshold, the 10th point as plotted in figure 5 should fall below its correct level, and it should not be surprising that the ninth point would also do so.

The slope and position of the line drawn through the circular symbols for the first 8 mass groups call for $\alpha = 10^{-14.63}$ and $\beta = 1.34$, as nearly as can be estimated, in the mass distribution equation

$$F_{>} = \alpha m^{-\beta} \quad (24)$$

In that equation $F_{>}$ is influx rate of meteors of mass greater than m in particles per square meter per second. The value of β equal to 1.34 has previously been widely, though not universally, accepted. It is the value for the "Whipple 1963A" line (ref. 13) which is also shown in figure 5 for comparison. The close agreement, however, seems to be fortuitous. This same value was obtained by Hawkins and Upton (ref. 17), from whose work Whipple adopted the slope used for his 1963A line. But Hawkins and Upton used photographic magnitudes determined by Hawkins and Southworth (ref. 14). Kresak (ref. 18) has shown an appreciable systematic difference in the magnitude and mass scales obtained from references 6 and 14. As the mass values used in the present analysis were those of McCrosky and Posen (ref. 6), different results for the parameter β should be expected between the present analysis and that of Hawkins and Upton. With reference to existing dissent relative to the value 1.34, a value of β as low as 0.88 has been advanced by Dohnanyi (ref. 19).

The present analysis makes clear the fact that an accurate determination of the mass distribution throughout the photographic range is possible only with explicit use of, or implicit determination of an accurate weighting factor to correct the photographic bias due to differences of mass and velocity. Prior to reference 2, however, no extensive analysis appears to have been published in relation to any weighting factor to be used for this purpose. Although at least to some extent fortuitously, the value of β equal to 1.34 has been well confirmed by the present analysis, with use of the weighting factor from reference 2. Also, the straightness of the cumulative mass distribution curve on a full logarithmic plot has largely been demonstrated, whereas such straight-

ness had previously been effectively assumed except for the larger masses within the photographic range.

The use of the mass scale of McCrosky and Posen (ref. 6) herein and in reference 2 does not necessarily involve a preference for this scale relative to that of reference 14. This choice was only a matter of convenience. The weighting factor derived in reference 2 would be supported by the present analysis, even if the mass used here were not correct, so long as the mass used was a monotonic increasing function of the true mass alone. If the mass used here were a power of the true mass times a constant, the value of β derived here could be readily adjusted.

The value of α for the "Whipple 1963A" line is $10^{-14.18}$, somewhat higher than the value $10^{-14.63}$ from this analysis. The lower level from this analysis is believed to be roughly the same as might be expected because of the correction for the effect of gravitational focussing. The Whipple line is without an adjustment for gravitational focussing. Also, for the line shown, the value of α used by Whipple has been multiplied by two to eliminate his Earth shielding factor.

At first thought, an assumption might be made that the results of this analysis should have indicated a substantially greater influx than had previously been thought to exist. For, the analysis shows a much greater number of meteoroids of low velocity relative to those of higher velocity. The additional meteoroids at low velocity might be considered as additive to those that had previously been counted. However, by study of figure 5, it may be seen that such is not the case. By previous methods, only the two or three lowest plotted points would have appeared as lying within a straight line with a slope corresponding to a value of $\beta = 1.34$. All the other plotted points would have fallen off below that line. By previous methods it was essentially assumed that such fall-off was due to failure of observation of faint meteors and the slope for the straight line was based on the lowest points. But as even the slowest meteoroids were observed for the largest masses, approximately the proper slope and the proper level of the line had been determined on the basis of those lowest points.

Hence, the establishment of a substantially reduced average geocentric velocity of meteoroids in this analysis is actually in harmony with the previous concept as to mass distribution and influx rate, and it reinforces that concept by the demonstration that a straight-line relation actually does exist at least for the eight heaviest of the 10 mass groups analyzed.

CONCLUDING REMARKS

After completion of the analysis that has been presented herein, references 20 and 21 came to the author's attention. In reference 20, Erickson derived a velocity histogram that closely resembles the adjusted velocity histogram for all masses presented

herein, with an average velocity of 16.5 kilometers per second (2.7 km/sec greater than the value derived herein). His method was roughly complementary to that used herein, inasmuch as he divided the meteor sample into velocity groups rather than mass groups. In reference 21, Dohnanyi showed a similar "semi-empirical" distribution of velocity v_{∞} , differing from that obtained herein for velocity v_G only slightly more than Erickson's distribution. Dohnanyi's average velocity is 19.2 kilometers per second.

The weighting factor that was developed in reference 2 is supported by the general agreement of a histogram for unaccelerated velocity of all meteors, adjusted by that weighting factor, with an unadjusted histogram for unaccelerated velocity of heavy meteors. That agreement, considered together with the partial agreement of the adjusted histogram for all masses with the unadjusted histograms for 10 mass groups, supports the assumption of a single velocity distribution for all masses within the photographic range. Also, the analysis for cumulative mass distribution shows a linear relation on a full logarithmic plot.

It is true that the assumption of a single-velocity distribution for all masses as well as the straight-line relation and the value of $\beta = 1.34$ were used in the derivation of the weighting factor in reference 2. In appendix E an argument is presented that each of these assumptions is confirmed independently of their use as assumptions in reference 2. Hence, the results of the present analysis are of major value in establishing the dependability of the weighting factor. At the same time, the establishment of a basis for confidence in the weighting factor automatically establishes a basis for confidence in the average unaccelerated geocentric velocity of about 13.8 kilometers per second obtained with its use. This average velocity (not greatly different from the averages of Dohnanyi and Erickson) is less than half the raw average of 30 kilometers per second, which has had much use. The greatly reduced average velocity should have an important effect on estimates of necessary armor thickness. Further study in this connection would seem to be well justified.

As stated in reference 2, dissension exists as to whether luminous efficiency is proportional to meteoroid velocity relative to Earth's atmosphere. The weighting factor $\phi_{w(1)}$ was derived on that basis. In appendix F an argument is presented that the present analysis tends to support the linear dependence of luminous efficiency on velocity.

Lewis Research Center,
National Aeronautics and Space Administration,
Cleveland, Ohio, November 21, 1968,
120-27-04-36-22.

APPENDIX A

SYMBOLS

A	effective capture cross section of Earth for meteoroids (larger than Earth's cross section because of gravity focussing)
a	constant used with varying significance as made clear in context
b	constant used with varying significance as made clear in context
$C_{a(i)}$	count of meteors within mass group i , adjusted only for effect of gravitational focussing
$C_{cum(i)}$	fully corrected cumulative count for influx of meteoroids of mass greater than lower limit for mass group i as defined by eq. (20), particles $m^{-2} sec^{-1}$
C_i	fully corrected count of meteoroids within mass group i defined by eq. (18)
C'_i	tentatively corrected count of meteoroids within mass group as defined in eq. (15), particles $m^{-2} sec^{-1}$
c	constant used with varying significance as made clear in the context; also, particle flux at infinite distance from Earth, as used in eqs. (B1) and (B2)
$F(Z_R)_{av}$	statistical function of zenith angle of meteor and position of meteor within field of view of cameras, explained in detail in ref. 2, nondimensional
$F_{>}$	influx rate of meteoroids of mass greater than specified value m , particles $m^{-2} sec^{-1}$
$f(v_G)$	frequency of occurrence of meteors of geocentric velocity v_G as defined in eq. (C3)
n	subscript for the symbol $\varphi_{W(n)}$, equal to 1, 2, 3, or 4, and indicating that the symbol is defined by the equation of that number
r_A	radius of a circle of area A , km
r_E	radius of Earth, km
v_e	velocity of escape from Earth at position where meteoroid impacts Earth atmosphere, km/sec
v_G	velocity meteoroid would have had relative to Earth if Earth's gravity had not affected that velocity, km/sec

- v_{∞} velocity of meteoroid relative to Earth atmosphere at position of first infinitesimal encounter with atmosphere, km/sec
- v'_{∞} hypothetical geocentric velocity of particle at infinite distance from Earth, km/sec
- x distance from y-y axis in pair of rectangular coordinates, used with varying significance as made clear in the context.
- y distance from x-x axis in pair of rectangular coordinates used with varying significance as made clear in the context
- Z_R angle of path of meteor to zenith, deg or rad
- α factor of proportionality in eq. (24)
- α° factor of proportionality evaluated in eq. (11)
- β exponent of mass m in eq. (24) for influx rate of meteoroids
- $\varphi_{w(n)}$ weighting factor defined in equation having number indicated by subscript n , nondimensional
- $\varphi_{(i)}$ revised correcting factor for counts of meteors within mass group i defined by eq. (17)
- $\varphi'_{(i)}$ correcting factor for counts of meteors within mass group i (identical with φ of appendix C)

APPENDIX B

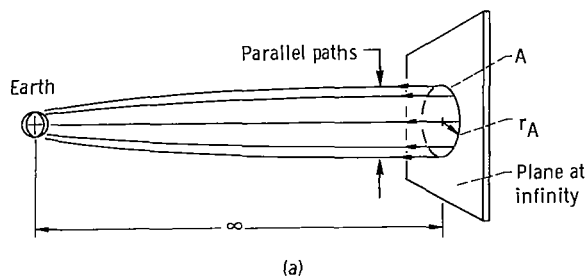
DEVELOPMENT OF EQUATION FOR GRAVITY-FOCUSSING ADJUSTMENT

Shelton, Stern, and Hale (ref. 7) present the following equation as governing the effect of gravity focussing

$$\frac{I_E}{\pi r_E^2 c} = 1 + \frac{v_e^2}{v_\infty'^2} \quad (B1)$$

where I_E is number of particles intercepted by Earth, r_E is radius of Earth and atmosphere, c is particle flux per unit area at infinity (in parallel paths), v_e is velocity of escape from Earth, and v_∞' is particle velocity at infinity, primed here to avoid confusion with another significance assigned to v_∞ in the main text. With the aid of equation (B1), an adjusting factor may readily be formulated for use in the main text to adjust an actual count of particles at any particular geocentric velocity, as observed within the atmosphere of Earth, to yield a value that would properly apply to a gravity-free Earth. Such an adjusted count would apply to a space radiator located approximately in a position along the path of Earth in its orbit, but at a position far from Earth. Before such adjusting factor is formulated, however, a verification of the applicability of equation (B1) will be undertaken.

In the derivation of equation (B1) in reference 7, the gravitational influence of the sun was ignored and particles were treated as emanating perpendicularly from a circular area such as A within a plane surface located at an infinite distance from Earth (see sketch (a)). The reality, of course, is that particles approach the Earth in orbits



that are conic sections having foci at the center of the sun. With neglect of the sun's influence, the ratio of the number of particles reaching Earth to the number that would have reached Earth without the effect of Earth gravity would be the ratio of the area A in sketch (a) to the projected area of the Earth and its atmosphere. But, if equation (B1) is correct, then this same ratio should be equal to the left-hand side of equation (B1). Hence, from equation (B1), rewritten as

$$\frac{\pi r_A^2 c}{\pi r_E^2 c} = 1 + \frac{v_e^2}{v_\infty'^2} \quad (\text{B2})$$

a ratio of radii may be expressed as

$$\frac{r_A}{r_E} = \sqrt{1 + \left(\frac{v_e}{v_\infty'}\right)^2} \quad (\text{B3})$$

where r_A is the radius of the circular area A .

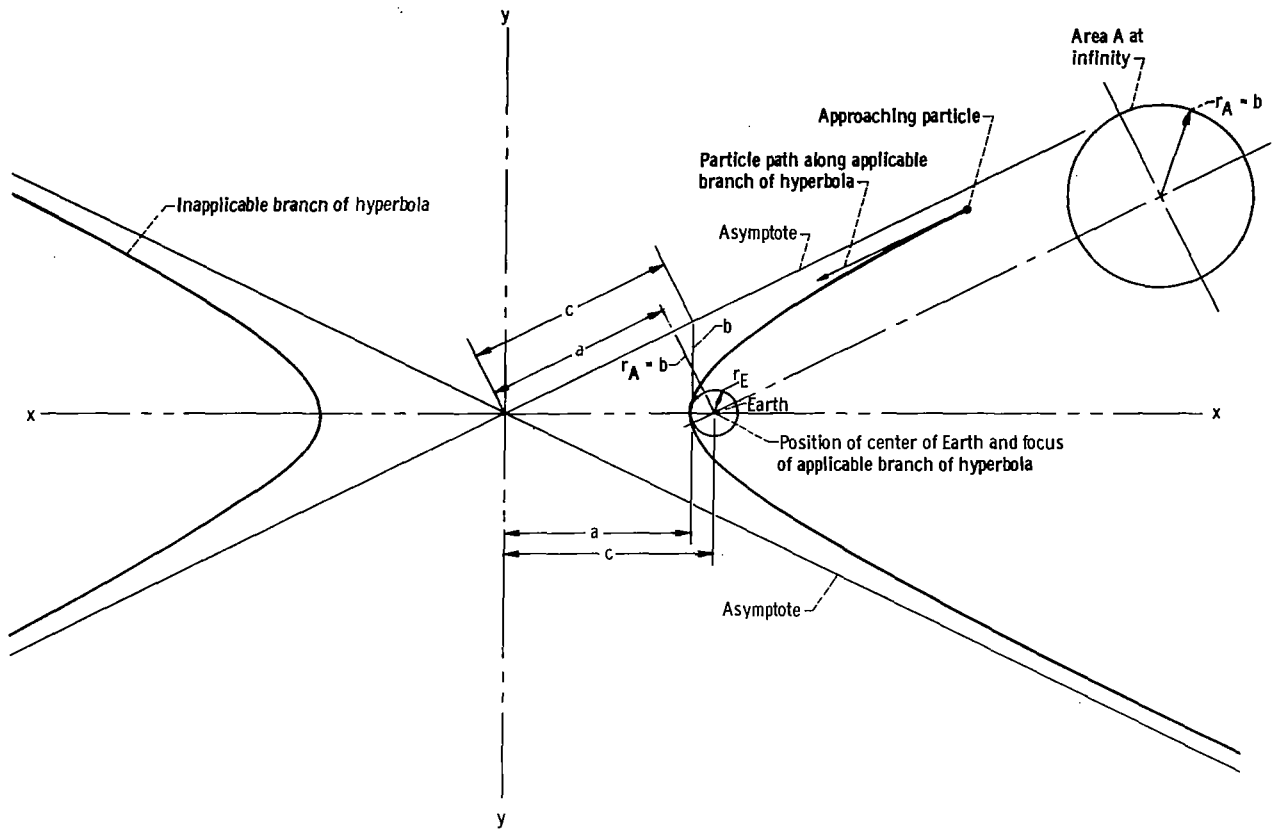
Equation (B3) can easily be derived for the condition assumed, with reference to figure 6. As circular symmetry exists about an axis extending from Earth's center to the center of the circular area A , it is necessary to consider only a single particle, leaving some point within the perimeter of the area A in a direction parallel to the axis of symmetry. Such a particle, being marginal from the standpoint of collision with Earth's atmosphere, should just graze the atmosphere tangentially. It is well known that a particle at an infinite distance from and having a component of velocity toward an attractive center will approach that center along one branch of a hyperbola having that center as its focus. This condition is illustrated in the figure. The hyperbolic orbit is assumed to be symmetrical relative to an x axis with origin midway between the two branches of the hyperbola.

The general equation for such a hyperbola is

$$\frac{x^2}{a^2} - \frac{y^2}{b^2} = 1 \quad (\text{B4})$$

where a and b are constants. It is well known that

$$a^2 + b^2 = c^2 \quad (\text{B5})$$



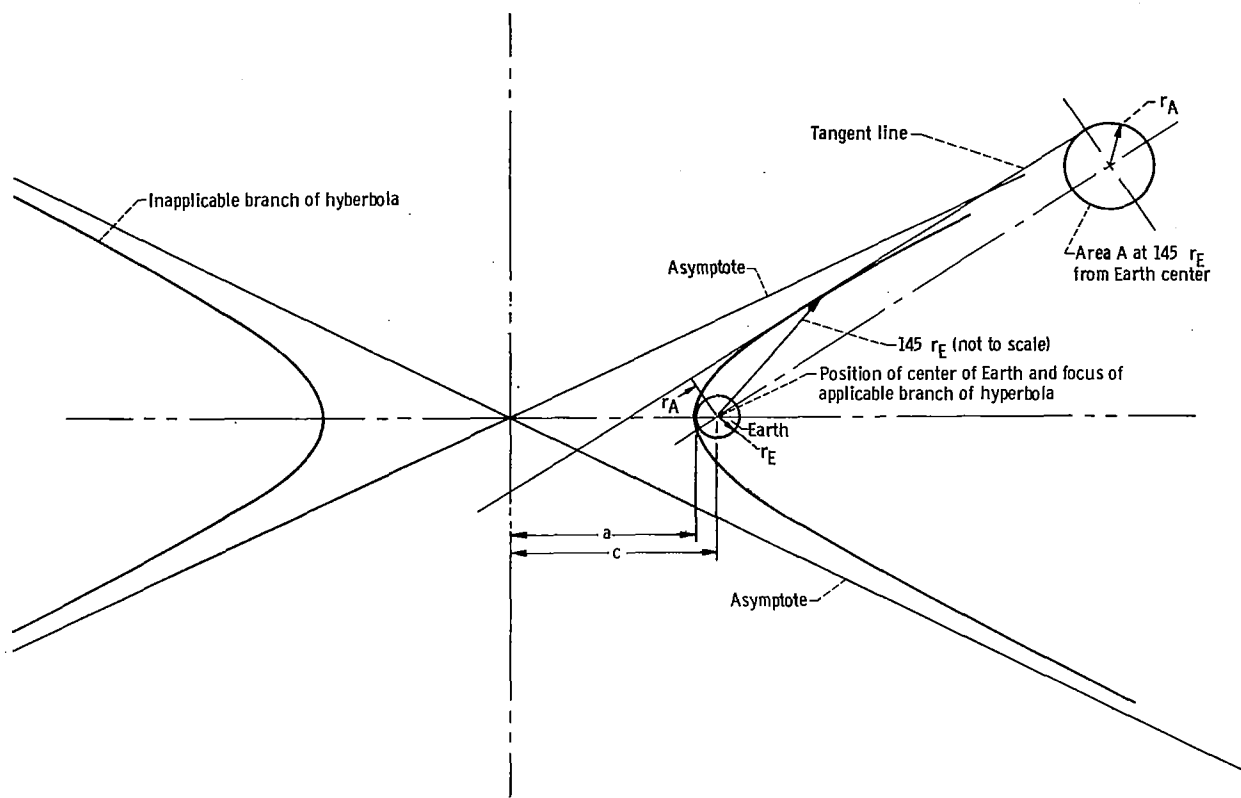
(a) Sun's gravitation neglected.

Figure 6. - Effective capture area of Earth for slow particle.

where c is the distance from origin to the focus of either branch of the hyperbola. The physical significance of a , b , and c , as shown by either of the two congruent right triangles in figure 6(a), is also well known (see any textbook in analytic geometry). From the figure it is seen that r_A is equal to b . The values of a and b may be determined from conditions that must exist at perigee, the point where the applicable branch of the hyperbola intersects the x axis. Those conditions are that (1) the marginal particle must reach a minimum distance from the center of Earth equal to r_E , (2) the gravitational and centrifugal forces acting on the particle must extend in exactly opposite directions, and (3) because of item (2), the gravitational and centrifugal forces must be equal.

A foundation has now been laid for derivation of equation (B3), the equivalent of equation (B1). The derivation may be simply performed with use of well known principles of physics and analytic geometry. The details are omitted.

Difficulty is encountered in a rigid demonstration that equation (B1), (B2), or (B3) applies even approximately to the real condition involving the sun's influence. However,



(b) Sun's gravitation considered.
Figure 6. - Concluded.

it can be shown that application of these equations is reasonably consistent with a method of approximate solution of the 3-body problem that has given good results in practice.

Knip and Zola (ref. 23) have shown that good approximate solutions are obtained by the following method for trajectories of small objects from positions near Earth to positions far from Earth or the reverse. Here the expression "near Earth" applies to positions such that the gravitational influence of the sun is negligible compared with that of Earth. The expression "far from Earth" applies to positions such that the gravitational influence of Earth is negligible compared with that of the sun. The method is composed of the following procedures: (1) a "sphere of influence" of Earth is defined as a moving sphere in space, always concentric with Earth's spherical surface, and having a radius equal to 145 Earth radii, (2) when the small object is within Earth's sphere of influence, it is treated as being affected by Earth's gravitation alone, except that the motion of the object is defined relative to a coordinate system with origin at Earth center and moving with Earth center in orbit about the sun, (3) when the small object is outside Earth's sphere of influence, it is treated as being affected by the sun's gravitation only, and (4) when the small object passes into or out of Earth's sphere of

influence, the velocity and direction of motion are treated as unchanged relative to either Earth or sun.

In application of the method described to the gravity focussing effect, it is necessary to consider particles entering Earth's sphere of influence in parallel paths at a given velocity. The condition is illustrated in figure 6(b). For the same value of v'_{∞} , the hyperbolic orbit is exactly as in figure 6(a). However, a marginal particle, destined to graze the Earth atmosphere, will enter the Earth sphere of influence traveling in a direction tangent to the hyperbolic orbit at the distance of 145 Earth radii from Earth center. If thereafter it traveled an undeflected path, it would follow the tangent line and would cross over the x axis at a position to the right of the origin. The circular source area A must now be treated as at a distance of 145 Earth radii from Earth center rather than at an infinite distance. A particle emanating from its center, in a direction parallel to the tangent line, would follow a straight-line path toward Earth center. Hence, the radius r_A of the source area A must now be the perpendicular distance of the tangent line from Earth center. With the newly defined value of r_A , the concentration ratio due to the focussing effect of gravity would still be expressed by the left-hand side of equation (B3), but not by the right-hand side of that equation.

No analytical expression has been found to substitute for the right-hand side of equation (B3). However, for any particular value of v'_{∞} a value of the concentration ratio $(r_A/r_E)^2$ may be readily calculated with use of elementary principles of analytic geometry. For example, with $v'_{\infty} = 1.0$ kilometers per second the value of $(r_A/r_E)^2$ may be calculated as 67.15. For the same value of v'_{∞} , equation (B2) gives a value 124.21. Hence, it is seen that equation (B1) or (B2) would provide too large a concentration ratio by approximately 85 percent for $v'_{\infty} = 1$ kilometer per second, if the sphere-of-influence treatment were considered to be strictly correct.

Computations and comparisons were made in the manner described for each integral value of v'_{∞} from 1 to 80 kilometers per second. The results, in percentage overestimate by equation (B1) or (B2), in comparison with the sphere-of-influence treatment, are plotted in figure 7. The percentage overestimate reduces to less than 4 percent at a velocity $v'_{\infty} = 5$ kilometers per second. But, in figure 1, it is seen that particles with values of $v'_{\infty} = 5$ kilometers per second or less are only a small fraction of the total.

From the foregoing treatment, it appears that use of equation (B1) is well justified for the purposes of the analysis conducted in the main text. Accordingly, suitable adjusting factors $\phi_{w(2)}$ and $\phi_{w(3)}$ will now be formulated on the basis of that equation. The desired factors will operate on the flux within Earth atmosphere observed at a given value of v'_{∞} , with and without adjustment for the photographic bias of meteoroid mass and velocity, to produce a flux as it would exist without gravitational focussing. If c represents the flux corrected for the effect of gravitational focussing and c_{ob} represents the observed flux, with or without the adjustment for mass and velocity,

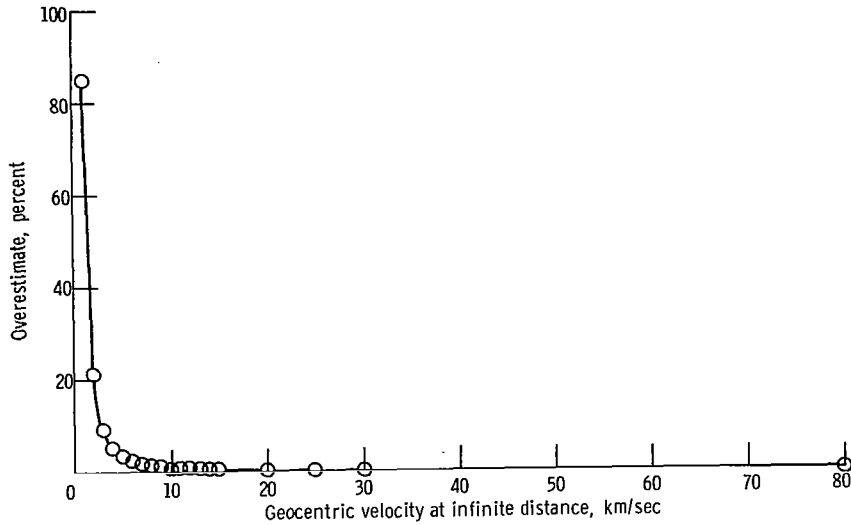


Figure 7. - Calculated overestimates of effect of gravitational focussing by neglect of sun's gravitation.

then

$$c_{ob} = \frac{\pi r_A^2 c}{\pi r_E^2} \quad (B6)$$

From equations (B2) and (B6),

$$\frac{c_{ob}}{c} = 1 + \left(\frac{v_e}{v_\infty'} \right)^2 \quad (B7)$$

or

$$c = \frac{c_{ob}}{\left[1 + \left(\frac{v_e}{v_\infty'} \right)^2 \right]} \quad (B8)$$

Now, in the main text, a weighting factor $\phi_{w(1)}$ is expressed in equation (1), by which an actual count of particles at any particular velocity may be multiplied to yield a value corrected for mass and velocity bias, and a weighting factor $\phi_{w(4)}$ equal to unity is shown by equation (4), use of which in the computer program leaves the actual

count unaffected. If the actual count is designated c'_{ob} , then application of the factor $\varphi_{w(1)}$ or $\varphi_{w(4)}$ yields

$$c_{ob} = c'_{ob}\varphi_{w(1)} \quad (B9)$$

or

$$c_{ob} = c'_{ob}\varphi_{w(4)}$$

in which c_{ob} is a count that may be substituted into equation (B8) to yield a count c corrected for the gravity focussing effect. Revised correcting factors $\varphi_{w(2)}$ and $\varphi_{w(3)}$ will now be defined, such that

$$\left. \begin{aligned} c &= c'_{ob}\varphi'_{w(2)} \\ c &= c'_{ob}\varphi'_{w(3)} \end{aligned} \right\} \quad (B10)$$

Then, from equations (B8) to (B10),

$$\left. \begin{aligned} \frac{c}{c'_{ob}} &= \left[1 + \left(\frac{v_e}{v'_{\infty}} \right)^2 \right]^{-1} \varphi_{w(1)} \\ \frac{c}{c'_{ob}} &= \left[1 + \left(\frac{v_e}{v'_{\infty}} \right)^2 \right]^{-1} \varphi_{w(4)} \end{aligned} \right\} \quad (B11)$$

Now, in the main text, v_G is equivalent to v_{∞}' as used in this appendix. If such substitution is made in equations (B11), and if the values of $\varphi_{w(1)}$ and $\varphi_{w(4)}$ from equations (1) and (4) are also substituted, equations (B11) express as c/c'_{ob} the weighting factor $\varphi_{w(2)}$ of equation (2) or $\varphi_{w(3)}$ of equation (3).

APPENDIX C

DEVELOPMENT OF OFFSET LOG-NORMAL EQUATION FOR VELOCITY DISTRIBUTION OF METEORIODS

The curve in figure 2 is a parabola centered on the y axis as shown. The equation of that parabola is

$$x = \pm 0.409 \sqrt{-y} \quad (C1)$$

where x and y are linear distances measured from the axes x-x and y-y as shown, in a unit equal to log 10 as plotted on the full logarithmic chart. It can readily be shown that this parabola represents a log-normal velocity distribution, offset 1.5 kilometers per second toward higher velocities (ref 8).

Choice of a unit of length equal to log 10, for convenience, in the formulation of equation (C1) and in the construction of the parabola in figure 2 commits equation (C1) to sue only in conjunction with logarithms to the base 10. For it is only to the base 10 that log 10 can have a value of unity. In the measurement of x and y in figure 2, the unit of length $\log_{10} 10$ is greater than the unit of length $\log_e e$ by the factor $\log_e 10$, because in the first case the distance from 1 to 10 on the logarithmic scale is the unit of length, while in the second case the distance from 1 to e on the logarithmic scale is the unit of length. If x and y in equation (C1) each have the dimension l, then the constant 0.409 must have the dimension $l^{1/2}$. Hence, if the unit of l is changed by a factor $(\log_e 10)^{-1}$, the value of the constant 0.409 must be multiplied by the one-half power of the reciprocal of that factor. Accordingly, equation (C1) must be changed to

$$x = \pm 0.409 \sqrt{\log_e 10} \sqrt{-y} \quad (C2)$$

Equation (C2), then, may be used in conjunction with natural logarithms.

The standard equation for a normal distribution of velocity v_G would be

$$f(v_G) = a \cdot \exp \left[-\frac{1}{2} \left(\frac{v_G - b}{c} \right)^2 \right] \quad (C3)$$

where $f(v_G)$ represents the frequency of occurrence of any velocity v_G in terms of fraction of total population having velocity $v_G \pm \frac{1}{2} dv_G$, divided by dv_G , and where a, b, and c are constants. For a log-normal distribution in terms of v_G (offset 1.5 km/sec)

equation (C3) becomes

$$f(v_G) = a \cdot \exp \left\{ -\frac{1}{2} \left[\frac{\log_e(v_G + 1.5) - \log_e b}{c} \right]^2 \right\} \quad (C4)$$

or

$$\log_e f(v_G) = \log_e a - \frac{1}{2} \left[\frac{\log_e(v_G + 1.5) - \log_e b}{c} \right]^2 \quad (C5)$$

or

$$\log_e(v_G + 1.5) - \log_e b = \sqrt{2} c [\log_e a - \log_e f(v_G)]^{1/2} \quad (C6)$$

Now if the x-x axis is located at an ordinate value equal to $\log a$ and the y-y axis is located at an abscissa value of $\log b$ (both on the full logarithmic plot of fig. 2) and if the values of x and y are measured linearly from these axis, in units equal to $\log_e e$ on the scale of figure 2, then

$$x = \log_e(v_G + 1.5) - \log_e b \quad (C7)$$

and

$$y = \log_e f(v_G) - \log_e a \quad (C8)$$

With substitution of x and y from equations (C7) and (C8), equation (C6) becomes

$$x = \pm \sqrt{2} c \sqrt{-y} \quad (C9)$$

By comparison of equation (C9) with equation (C2), it is seen that

$$c = 0.409 \frac{\sqrt{\log_e 10}}{\sqrt{2}} = 0.44 \quad (C10)$$

From the positions of the x and y axes in figure 2 and with use of a fractional value rather than percentage value for frequency,

$$\log_e a = \log_e 0.07 \quad (C11)$$

and

$$\log_e b = \log_e 11.7 \quad (\text{C12})$$

Finally, equation (B13) may be written from equations (C4) and (C10) to (C12).

APPENDIX D

ADJUSTING FACTOR FOR COUNT OF METEORS WITHIN A MASS GROUP

It will be demonstrated that a valid adjusting factor for a count of meteors within a particular mass range is obtained as the antilogarithm of the vertical shift necessary to bring the higher-velocity regions of an unadjusted velocity distribution for the mass group into agreement with the correct distribution, when both distributions are plotted on a semilogarithmic scale, as in the case of figure 3(e).

Within a given mass group, let $f_o(v_1)$ be the observed fraction of the observed total count, and let $f_r(v_1)$ be the correct fraction of the correct total count of meteors having velocities within the interval $v_1 \pm \delta$, where δ is some small number. Assume v_1 is high enough that no meteors within the mass group and within the velocity range $v_1 + \delta$ will go unobserved because of faint luminosity. Then

$$k_o = k_r \quad (D1)$$

where k_o is the observed number of meteors and k_r is the correct number within the mass group and within the velocity interval $v_1 \pm \delta$.

Let A_o be the total observed count and A_r be the total correct count for the mass group. Then

$$f_o(v_1) = \frac{k_o}{A_o} \quad (D2)$$

$$f_r(v_1) = \frac{k_r}{A_r} \quad (D3)$$

Now, the desired adjusting factor, by which A_o should be multiplied to obtain A_r , is

$$\varphi = \frac{A_r}{A_o} \quad (D4)$$

From equations (D2) to (D4),

$$\varphi = \frac{f_o(v_1) k_r}{f_r(v_1) k_o} \quad (D5)$$

From equations (D1) and (D5),

$$\varphi = \frac{f_o(v_1)}{f_r(v_1)} \quad (D6)$$

or

$$\log \varphi = \log f_o(v_1) - \log f_r(v_1) \quad (D7)$$

For semilogarithmic plots, equation (D7) indicates that, for any velocity v_1 where the observed count is correct, the needed adjusting factor will be the difference in level of the observed and correct curves at that velocity v_1 . Hence, if theoretical reason exists to believe that the observed count is correct throughout a particular velocity region, then the logarithm of the desired adjusting factor can be obtained by measuring the vertical shift required to bring the observed distribution curve into agreement with the correct curve throughout that velocity region.

But good reason has been given to expect that the observed curves will be correct throughout the velocity region above some critical value at or above which failure to observe meteors would not occur for the mass group. Hence the method should be applicable in the comparisons used in the main text.

APPENDIX E

EFFECTS OF ASSUMPTIONS REGARDING MASS AND VELOCITY DISTRIBUTIONS

A question of circular logic exists in the indication that $\beta = 1.34$ in figure 5 and the indication of identical velocity distributions for different masses in figures 3(a) to (i). Both these conditions were assumed in the development of the weighting factor $\varphi_{w(1)}$ of equation (1) (eq. (75) of ref. 2).

Mass Distribution

Consideration will now be given to the question whether an iterative procedure that could be performed would converge to a value of approximately 1.34 for β . That procedure would involve repetitions of the work shown in reference 2 (pp. 31 to 34) and the work presented in this paper between equations (1) and (24). In each repetition, the value of β obtained from the preceding repetition would be used as a starting value in reference 2 (p. 31). Comparisons of histograms would be made in a new figure 3, and a new figure 5 would be constructed.

The suggested iterative procedure would be excessively long and laborious. However, the question of convergence to a value of β near 1.34 can be examined without the need of actually performing the procedure, as follows.

In description of some details of the iterative process, the factors $(\cos Z_R)^{-0.196}$ and $F(Z_R)_{av}^{0.730}$ in equation (1) will be omitted, because an adjusted histogram for all masses (not shown in this report) with the weighting factor according to the equation

$$\varphi'_{w(1)} = v_{\infty}^{-4.22} \quad (E1)$$

does not differ appreciably from the adjusted histogram for all masses obtained with $\varphi_{w(1)}$ according to equation (1).

In the analysis that has been reported here, in determining the value of β , the author depended on physical measurement of slope from a carefully constructed full-logarithmic plot, which has been reproduced as figure 5. This method was preferred to a least-squares fit because it allowed judgment in weighting of the plotted point for mass group 8 with allowance for the possibility that the fall-off evident for mass groups 9 and 10 may actually have started with group 8. But, for the purpose of examining the question of convergence, a rigid mathematical determination of slope will be needed even if it does not necessarily give the best result. For that purpose, the straight line providing a least-squares fit to the data will be used for the first eight mass groups. Groups 9 and

10 will be disregarded. For the data shown in table II and plotted in figure 5, such a least-squares fit was obtained with a slope of -1.32, which is only 0.02 different from that determined visually.

Now, as an example, if a value of $\beta = 1.25$ had been assumed between equations (59) and (60) in reference 2, then the exponent of v_∞ in equation (75) would have been -3.96. The lower absolute value of this exponent would have changed the shape of the adjusted velocity distribution for all masses used for the comparisons in figure 3. But the change in shape would not have been enough to prevent the comparisons, as will be explained. Also, the effect of the changed assumption regarding β on figure 5 will be estimated.

In the comparisons, instead of the adjusted histogram for all masses, use could have been made of a smooth curve representing $f(v_G)$ according to equation (5) (times 100). Some analogous smooth curve would exist with use of a weighting factor like $\varphi'_{w(1)}$ of equation (E1) but with the exponent -3.96. Relative influx rates shown by that analogous smooth curve would be proportional to those given by equation (5), but multiplied by $v_\infty^{(4.22-3.96)}$ or $v_\infty^{0.26}$.

Now, with mass group 5 as an example, it is seen that the agreement in shape of the two histograms in figure 3(e) occurs approximately within the region of values of v_G from 28 to 58 kilometers per second. (Hereinafter, for any mass group i , the range of v_G within which the shape of the histograms agree will be referred to as the matching range.) The analogous smooth curve for the assumption $\beta = 1.25$ would not fit the raw histogram in this figure within the matching range so well, but it could have been fitted approximately, with a cross over somewhere within the matching range (values of v_G from 28 to 58 km/sec).

The percentage of total influx of meteoroids shown by the analogous smooth curve at any velocity $v_G \pm 0.5$ kilometers per second must be given very closely by the equation

$$f'(v_G) (\%) = 100 \times \frac{\exp \left\{ -\frac{1}{2} \left[\frac{\log_e (v_G + 1.5) - \log_e 11.7}{0.44} \right]^2 \right\} \left[\sqrt{v_G^2 + 121} \right]^{0.26}}{\sum_{i=1}^{80} \exp \left\{ -\frac{1}{2} \left[\frac{\log_e (i + 1) - \log_e 11.7}{0.44} \right]^2 \right\} \left[\sqrt{(i - 0.5)^2 + 121} \right]^{0.26}} \quad (\text{E2})$$

Equation (E2) indicates an influx of 0.888 and 0.0104 percent of the total with velocities v_G at 28 and 58 kilometers per second, respectively, which are higher on the logarithmic scale than the values 0.771 and 0.00757 percent given by equation (5) by distances equal to $\log(1.152)$ and $\log(1.374)$. Hence, the analogous smooth curve for the assumed $\beta = 1.25$ would require a smaller shift to produce approximate agreement with the raw histogram within the matching range for mass group 5 by a distance approx-

imately equal to the average of $\log(1.152)$ and $\log(1.374)$, that is, by the distance $\log(1.258)$. Accordingly, the shift $\varphi'_{(5)}$ in table I would be reduced from $\log(6.70)$ to $\log(6.70/1.258)$, or $\log(5.326)$. (Hereinafter for any mass group i the reduction of shift, like $\log(1.258)$ for $i = 5$, will be called the shift decrement.)

Similarly, $\varphi'_{(1)}$ and $\varphi'_{(2)}$ in table I would become $\log(1.32)$ and $\log(1.14)$, the last term in equation (17) would become $-\log(1.223)$, the corrected shift $\varphi_{(5)}$ in table II would become $\log(4.36)$, and the fully corrected count C_5 would become 1.72×10^{-14} .

Reduced values of C_i were also found in the same manner for mass groups 1 to 4 and 6 to 8. The resulting fully corrected cumulative counts $C_{\text{cum}(i)}$ for groups 1 to 8, were 3.94, 7.22, 14.66, 27.46, 44.66, 86.81, 167.5, and 346.5, all multiplied by 10^{-15} . The straight line providing the least-squares fit to the logarithms of these data has a slope of -1.27 , only 0.05 different from the result of -1.32 for the data in table II. But, as the new assumed value of $\beta = 1.25$ is less than the old assumed value $\beta = 1.34$ by 0.09, it may be seen that convergence has occurred by 44.5 percent of the difference between the two assumed values.

The foregoing procedure was also performed with an assumption $\beta = 1.43$. In this case, shift increments occurred instead of shift decrements. The resulting values of corrected cumulative counts for mass groups 1 to 8 were 3.94, 7.22, 16.07, 31.36, 52.33, 112.3, 224.5, and 484.0, all multiplied by 10^{-15} . The straight line providing the least-squares fit in this case has a slope of -1.38 . Here, convergence occurred by 33.3 percent of the difference between the assumed $\beta = 1.43$ and the original value $\beta = 1.34$.

The three pairs of values (assumed β equal to 1.25, 1.34, and 1.43, with resulting indicated values by least squares of 1.27, 1.32, and 1.38) indicate that convergence would occur to a value of 1.30. With indicated values by the graphical method in each case higher by 0.02, the indicated values of β for the three cases would be 1.29, 1.34, and 1.40, and the indicated value to which convergence would occur is very closely 1.34.

It may now be seen that convergence occurs for the following reasons:

(1) If the comparisons of histograms had involved the same matching range for all mass groups, then assumption of $\beta = 1.25$ (or any other value) would have decreased all values of $\log \varphi'_{(i)}$ by the same shift decrement; consequently, both terms in the right-hand side of equation (17) would have been decreased by the same amount. Hence all values of $\varphi_{(i)}$ from equation (17) would have been unchanged and no change would have occurred in any value of $C_{\text{cum}(i)}$. Any change in the values of $C_{\text{cum}(i)}$ and consequent change in indicated value of β would have to be caused by progressive change in the matching range and consequent progressive change in the shift decrement from one mass group to another.

(2) The increase in ordinate between mass groups $i - 1$ and i in figure 5 is equal to

$$\Delta \log C_{\text{cum}(i-1, i)} = \log \left[1 + \frac{C_i}{C_{\text{cum}(i-1)}} \right] \quad (\text{E3})$$

Any change in matching range between group (i - 1) and group i, with consequent change in shift decrement, may change the value of C_i and hence the value $\Delta \log C_{\text{cum}(i-1, i)}$. But note in table II that C_i and $C_{\text{cum}(i-1)}$ are generally nearly equal. Hence, the values of $C_{\text{cum}(i-2)}$, $C_{\text{cum}(i-3)}$, and so on, are comparatively unimportant parts of $C_{\text{cum}(i-1)}$ as it appears in equation (E3). Consequently, if a change in shift decrement occurs between groups (i-1) and i, then between groups i and (i+1) that changed shift decrement will apply almost as much to the denominator in equation (E3) as to the numerator. It follows that substantial changes in the value $\Delta \log C_{\text{cum}(i-1, i)}$ will occur only because of change in the shift decrement between groups (i-1) and i. The effect of that change in shift decrement will rapidly be lost for groups (i+1), (i+2), and so on.

(3) As an example, the value of β indicated by the interval between mass groups 4 and 5 only (from values in table II) is

$$\beta_{(4, 5)} = - \frac{\log_{10}(4.818 \times 10^{-14}) - \log_{10}(2.916 \times 10^{-14})}{\log_{10}(0.1025) - \log_{10}(0.1603)} = \frac{0.2181}{0.1942} = 1.123 \quad (\text{E4})$$

Now, from equation (E4), and by the reasoning in items (1) and (2), any change in shift decrement $\Delta D_{(4, 5)}$ between mass groups 4 and 5 will change the value of $\beta_{(4, 5)}$ to

$$\beta_{(4, 5)a} = \frac{0.2181 - \Delta D_{(4, 5)}}{0.1942} \quad (\text{E5})$$

or

$$\Delta \beta_{(4, 5)} = \beta_{(4, 5)a} - \beta_{(4, 5)} = \frac{-\Delta D_{(4, 5)}}{0.1942} \quad (\text{E6})$$

The median values of v_{c} within the matching range for groups 4 and 5 were 41 and 43 kilometers per second. The corresponding values of v_{∞} are 42.5 and 44.4 kilometers per second. Then, as the denominator of equation (E2) is constant, the change in shift decrement, by equations (5) and (E2), is

$$\Delta D_{(4,5)} = \log_{10} \left(\frac{44.4}{42.5} \right)^{0.26} = \log_{10}(1.045)^{0.26} = \log_{10}(1.012) \quad (\text{E7})$$

So, from equations (E6) and (E7)

$$\Delta \beta_{(4,5)} = -0.0267 \quad (\text{E8})$$

This result is about half the reduction 0.05 in the indicated value of β obtained by the least-squares fit for the first eight mass groups, probably because the change in median value of the matching range between mass groups 4 and 5 is somewhat less than in some of the other cases and because the conclusion in item (2) is only approximate.

(4) By review of the foregoing and the pertinent parts of reference 2, it may be seen that the exponent 0.26 in numerator and denominator of equation (E2) is equal to the factor 2.87 (ref. 2, eq. (59)) multiplied by the reduction of the assumed value of β (from 1.34 to 1.25 in this case); that is,

$$p = -2.87 \Delta \beta_a \quad (\text{E9})$$

where p is an exponent that might be substituted for 0.26 in equation (E2) and $\Delta \beta_a$ is a change in assumed value of β from the originally assumed value of 1.34. Hence, with any assumed value of β , the change in shift decrement between the fourth and fifth groups as an example would be given by the following modification of equation (E7)

$$\Delta D_{(4,5)} = \log_{10}(1.045)^{-2.87 \Delta \beta_a} \quad (\text{E10})$$

and from equations (E6) and (E10) the change of indicated β would be, approximately,

$$\Delta \beta_{(4,5)} = -\frac{1}{0.1942} \log_{10}(1.045)^{-2.87 \Delta \beta_a} = -0.28 \Delta \beta_a \quad (\text{E11})$$

Equation (E11) indicates that, whatever value of β had been assumed, for the interval between mass groups 4 and 5 convergence would have occurred about 72 percent of the way toward the value 1.32 as shown by the least-squares fit, or the value 1.34 obtained by the graphical method.

It appears now that the question of circularity is eliminated relative to the indicated value of β . It must still be examined regarding the matter of the same velocity distribution for different masses. The indication that $\beta = 1.34$ is still dependent on correctness of the assumption regarding uniformity of velocity distribution.

Velocity Distribution

As discussed earlier, the comparison of histograms in figure 3 does not agree exactly with the assumption of a single velocity distribution, as it affects values of v_G below about 20 kilometers per second in comparison with higher values. However, the assumption is not contradicted, even as an exact condition. Discussion here will be understood to apply only to velocity ranges in which confirmation exists by the comparisons in figure 3.

As a starting point for discussion, let it be supposed that the condition assumed actually does exist, just as shown by figures 3(a) and (b), for the two heaviest mass groups, and by figures 3(c) to (i) for other mass groups throughout the velocity region above a critical velocity in each case. All the histograms would then be correct as they are, because both assumptions used in the derivation of the weighting factor $\phi_{w(1)}$ are then satisfied.

Next let it be assumed that the influx rate, for the heaviest mass group only, is increased by an arbitrary percentage, but only throughout an arbitrary small velocity range from $v_{G(1)}$ to $v_{G(2)}$. The level of the raw histogram of mass group 1 will be raised, within the region from $v_{G(1)}$ to $v_{G(2)}$, by the same percentage as the increase in flux. But, regardless of the value of β , unless the range $v_{G(1)}$ to $v_{G(2)}$ lies in a region where the only incidence of meteors was within mass group 1, the level of the adjusted histogram for all masses, within that velocity region, will be raised by a smaller percentage. Hence, clearly the two histograms could not agree in shape after the change was made, even though the originally assumed condition would then be incorrect.

The same reasoning would apply to any part of the histogram for any mass group. It is apparent, therefore, with only minor exceptions, that change in the velocity distribution for any mass group would destroy the agreement of the histograms. Once the agreement was destroyed, it could be restored by changing the distributions for other mass groups, but only by changing in the same direction, that is, in the direction toward greater uniformity of the velocity distributions.

This reasoning is not dependent on the manner of derivation of $\phi_{w(1)}$, except in the primary assertion that the comparison of histograms would be as it is if the velocity distributions were the same for all mass groups.

APPENDIX F

RELATION OF LUMINOUS EFFICIENCY TO METEOROID VELOCITY

In reference 2 a relation was used

$$\tau = \tau_0 v \quad (\text{F1})$$

in which τ is luminous efficiency, v is instantaneous meteoroid velocity, and τ_0 is a constant. This assumption was involved in the derivation of equation (40) of reference 2, expressing a criterion for marginal exposure from the standpoint of discovery of a meteor on a photographic plate. Hence, it was involved in the derivation of ϕ_w of reference 2 (eq. (75)). As stated in reference 2, equation (F1), with τ_0 a constant, is by no means universally accepted. For that reason, the mutual relation between equation (F1), with constant τ_0 , and the present analysis will be discussed.

At least approximately τ_0 appears to be equal to a constant times v^n , where n is a positive or negative constant or is equal to zero as treated in reference 2. If this condition were substantially incorrect, then figure 4 of reference 2, for v_∞ as the sorted parameter, should have shown systematic variation of ordinate for various values of abscissa.

Now, let it be assumed that n is not actually equal to zero. Then, if τ_0 is redefined as a different constant than before, equation (F1) becomes

$$\tau = \tau_0 v^{n+1} \quad (\text{F2})$$

Then equation (40) of reference 2 becomes

$$C_{\text{marg}} = (m'_\infty)^{1.020} v_\infty^{2.842+n} (\cos Z_R)^{1.060} F(Z_R)^{-1} \quad (\text{F3})$$

Now, however, m'_∞ of equation (F3) cannot be the mass determined in reference 6. Relatively, without regard to absolute values, it must instead be

$$m'_\infty = m_\infty v^{-n} \quad (\text{F4})$$

where m_∞ is the mass shown in reference 6. Hence, in terms of m_∞ , equation (F3) becomes

$$C_{\text{marg}} = (m_{\infty} v^{-n})^{1.020} v_{\infty}^{2.842+n} (\cos Z_R)^{1.060} F(Z_R)^{-1}$$

$$= m_{\infty}^{1.020} v_{\infty}^{2.842-0.02n} (\cos Z_R)^{1.060} F(Z_R)^{-1} \quad (\text{F5})$$

which, if the absolute value of n is not greater than 1 or 2, is not significantly different from equation (40) of reference 2.

Now C_{marg} is a theoretically derived criterion for discovery of a meteor trace on a super Schmidt photographic plate. The ratio of the exponent of v_{∞} to the exponent of m_{∞} was confirmed closely in equation (45) of reference 2 by an empirical method. That method was based on 100 test meteors chosen in a manner not affected by m_{∞} or m'_{∞} . The method is as good for one value of n as another in equation (F4). But not so with the weighting factor φ_w of equation (75), which was developed in reference 2 (pp. 27 to 34) with use of equation (45) and other considerations. Of the other considerations, those pertinent here are

(1) the cumulative mass distribution

$$F_{>m} = \alpha m_{\infty}^{-\beta} \quad (\text{F6})$$

(2) the assumption that the velocity distribution $f(v_{\infty})$ (or $f(v_G)$) is the same for all values of m_{∞} .

Now it will appear later that equation (F6) may be used, with the same value of β , with m_{∞} or m'_{∞} . But validity of the assumption of the same velocity distribution for all values of m_{∞} , under the assumption that m'_{∞} is correct, needs some detailed consideration. For that purpose, alternative assumptions will be made as follows

(1) $f(v_{\infty})$ is independent of m'_{∞} .

(2) the cumulative frequency for m'_{∞} , $F_{>m'_{\infty}}$, for a particular value of v_{∞} is independent of that value of v_{∞} .

(Assumption (2) is a corollary of assumption (1)). Now the assumption actually used in reference 2, that $f(v_{\infty})$ is independent of m_{∞} , does not necessarily follow from the assumption that $f(v_{\infty})$ is independent of m'_{∞} . The fact that it does follow will have to be demonstrated.

Now assume any given value of m'_{∞} such as m_1 and any two values of v_{∞} such as v_1 and v_2 . Expressions may be written for two influx rates,

$$N(m_1, v_1) = f(v_1) F_{>m_1} = \alpha m_1^{-\beta} f(v_1) \quad (\text{F7})$$

and

$$N(m_1, v_2) = f(v_2) F_{>m_1} = \alpha m_1^{-\beta} f(v_2) \quad (\text{F8})$$

where $N(m_1, v_1)$ is the influx rate for particles of mass m'_∞ greater than m_1 and having velocity equal to v_1 and $N(m_1, v_2)$ is the same function for v_2 . Let

$$r' = \frac{N(m_1, v_2)}{N(m_1, v_1)} = \frac{f(v_2)}{f(v_1)} \quad (\text{F9})$$

Now consider a similar comparison in which m_∞ is kept constant instead of m'_∞ . In this comparison, let the first influx rate be $N(m_1, v_1)$ according to equation (F7) just as before. Then, for $N(m_1, v_1)$, the value of m_∞ according to equation (F4) will be

$$m_{\infty(1)} = m_1 v_1^n \quad (\text{F10})$$

For the second influx rate in this comparison let m'_∞ have a value m_2 such that the corresponding value of m_∞ will be identical with $m_{\infty(1)}$ of equation (F10), and let the velocity have the same value v_2 as in the earlier comparison. Then, from equations (F4) and (F10),

$$m_2 = m_{\infty(1)} v_2^{-n} = m_1 \left(\frac{v_1}{v_2} \right)^n \quad (\text{F11})$$

So,

$$N(m_2, v_2) = f(v_2) F_{>m_2} = \alpha m_2^{-\beta} f(v_2) = \alpha m_1^{-\beta} \left(\frac{v_1}{v_2} \right)^{-n\beta} f(v_2) \quad (\text{F12})$$

Hence, the new ratio of influx rates is

$$r = \frac{N(m_2, v_2)}{N(m_1, v_1)} = \left(\frac{v_1}{v_2} \right)^{-n\beta} \frac{f(v_2)}{f(v_1)} \quad (\text{F13})$$

Finally,

$$\frac{r}{r'} = \left(\frac{v_1}{v_2} \right)^{-n\beta} \quad (\text{F14})$$

Equation (F14) is free of both m'_∞ and m_∞ . It indicates that the ratio of influx rates at any two velocities is different with m'_∞ constant than with m_∞ constant, but nevertheless unchanging from one constant value of m_∞ to another.

Hence, the assumptions used in reference 2 (pp. 27 to 34) are valid, and equation (75) gives a theoretically correct expression for ϕ'_w , even if the values of m'_∞ are correct. It is only necessary to remember that the expression was derived on assumptions of uniform velocity distribution for all values of m_∞ and a value of $\beta = 1.34$ applying to the cumulative distribution of m_∞ . Hence, the validity of the weighting factor depends on confirmation of both those assumptions.

But it is argued in appendix E that both those assumptions are confirmed by the present analysis. Hence, within the accuracy of the method, it seems that $\phi_{w(1)}$ is a correct weighting factor, even under the assumption that n in equation (F4) is not equal to zero and under the corollary assumption that the correct mass is m'_∞ of equation (F4).

As far as has yet been shown, however, the value of β from figure 5 applies only to the values of m_∞ . That it must apply also to the values of m'_∞ may be seen as follows.

If the values m'_∞ are assumed correct, then the abscissa scale in figure 5 becomes $\log(m'_\infty v^n)$. Now consider arranging a parallel abscissa scale as $\log m'_\infty$. Consider in particular a value $m'_\infty = m_1$. As values of v_∞ did not go entirely to zero, any value of $m'_\infty = m_1$ in figure 5 must have lain within a region on the abscissa scale extending from

$$\log m_\infty = \log(m_1 v_{\min}^n) \quad (\text{F15})$$

to

$$\log m_\infty = \log(m_1 v_{\max}^n) \quad (\text{F16})$$

where v_{\min} and v_{\max} are the minimum and maximum values of v_∞ actually encountered. The range of this region on the abscissa scale then is

$$R(m_1) = \log(m_1 v_{\max}^n) - \log(m_1 v_{\min}^n) = \log\left(\frac{v_{\max}}{v_{\min}}\right)^n \quad (\text{F17})$$

It is seen that $R(m_1)$ is independent of the value of m_1 .

Now consider the distance between similar ends of the range for two values of m'_∞ such as m_1 and m_2 . This distance is

$$\Delta \log m'_\infty = \log(m_2 v_{\min}^n) - \log(m_1 v_{\min}^n) = \log\left(\frac{m_2}{m_1}\right) \quad (\text{F18})$$

But for the same two values of m'_∞ and again with the minimum value of v_∞ , the values of m_∞ according to equation (F4) are

$$m_{\infty(1)} = m_1 v_{\min}^n \quad (\text{F19})$$

$$m_{\infty(2)} = m_2 v_{\min}^n \quad (\text{F20})$$

the same as before, and the distance between these two values on the abscissa scale is

$$\Delta \log m_\infty = \log(m_2 v_{\min}^n) - \log(m_1 v_{\min}^n) = \log\left(\frac{m_2}{m_1}\right) \quad (\text{F21})$$

From equations (F18) and (F21), it is seen that the distance on the abscissa scale between m_1 and m_2 is the same as the distance between $m_{\infty(1)}$ and $m_{\infty(2)}$. Both scales are linear.

So the abscissa scale for m'_∞ (fig. 5) is the same as for m_∞ , except that an uncertainty always exists as to just where to put a value of $\log m'_\infty$ within a fixed range of values of $\log m_\infty$. The same uncertainty exists as to the ordinate, within the range of values shown in the figure for $\log(m'_\infty v_{\min})$ and $\log(m'_\infty v_{\max})$.

But, now, if the plot in figure 5 is assumed to extend from $m'_\infty = 0$ to $m'_\infty = \infty$, the limited uncertainty as to where to place each value of abscissa and ordinate becomes of no consequence relative to the slope of the line that will be produced. Note that this theoretical device is not vitiated by the fact that the value of β will not remain fixed outside the mass range actually represented in figure 5. Hence the value of β must

equal 1.34 for either m_{∞} or m'_{∞} .

Now, returning to reference 2, let it be supposed that equation (F2) had been used, with n not equal to zero. Suppose further that equation (F3) had been used instead of equation (40). Suppose that the mass values published in reference 6 had been the values of m'_{∞} instead of m_{∞} .

Then the empirical work between equations (40) and (45) should have confirmed equation (F3), just as it actually did confirm equation (40). But the work between equations (45) and (59) would have produced

$$\varphi_{\text{cor}} = F(v'_{\infty} Z_R)^{-\beta} [(2.842+n)/1.020] \quad (\text{F22})$$

Then, the work between equations (59) and (75) could have produced even approximately the same weighting factor φ_w as before only if a value of β very different from 1.34 had been used. As both the weighting factor and the value of β have already been confirmed (even for n not equal zero), it seems to follow that a correct weighting factor could not have been found with use of equation (F22).

At first thought, it may seem that both methods should be equally valid and that each should have its chance. Just as the value $\varphi_{w(1)}$ that was actually used is as valid for one condition as the other, then also equation (F22) and the replacement of equation (75) in reference 2 that would have been derived from it should also be valid for both cases.

But the new equation (75) would be valid for either case only if an analysis like that performed here confirmed, simultaneously, both the actual value of β used and the independence of velocity distribution on mass. As the present analysis did very closely confirm both those conditions, and did so simultaneously, it seems necessary to predict that use of a new equation for $\varphi_{w(1)}$, based on equation (F22), could not simultaneously confirm both conditions and that such a new weighting factor would therefore not be valid.

Hence, within the accuracy of the method, the present analysis seems to support equation (F1) with constant τ_0 . Slight departures from this condition, particularly if they involved only a gradual change in τ_0 approximately within the range of v_G below about 20 kilometers per second, would be possible. But, if later study shows that some low-velocity meteors were undiscovered within the heaviest mass groups, then the possibility of error in the assumption that τ_0 is constant will become even more restricted.

REFERENCES

1. Fish, R. H.; and Summers, J. L.: The Effect of Material Properties on Threshold Penetration. Proceedings of the Seventh Hypervelocity Impact Symposium, Vol. VI. Martin Co., Feb. 1965, pp. 1-26. (Available from DDC as AD-463232.)
2. Miller, C. D.: Simultaneous Correction of Velocity and Mass Bias in Photography of Meteors. NASA TR R-280, 1968.
3. Whipple, Fred L.: Photographic Meteor Orbits and Their Distribution in Space. *Astronom. J.* vol. 59, 1954, pp. 201-217.
4. Clough, Nestor; and Lieblein, Seymour: Significance of Photographic Meteor Data in the Design of Meteoroid Protection for Large Space Vehicles. NASA TN D-2958, 1965.
5. Whipple, Fred L.: Meteoritic Phenomena and Meteorites. *Physics and Medicine of the Upper Atmosphere.* Clayton S. White and Otis O. Benson, Jr., eds.. The University of New Mexico Press, 1952, ch. 10.
6. McCrosky, Richard E.; and Posen, Annette: Orbital Elements of Photographic Meteors. *Smithsonian Contributions to Astrophysics*, vol. 4, no. 2, 1961, pp. 15-84.
7. Shelton, R. D.; Stern, H. E.; and Hale, D. P.: Some Aspects of the Distribution of Meteoric Flux About an Attractive Center. *Space Research IV.* P. Muller, ed., Interscience Publ., 1964, pp. 875-907.
8. Bittker, David A.: Effect of Ambient Air Velocity on Atomization of Two Impinging Water Jets. NASA TN D-2087, 1964.
9. Wall, John K.: The Meteoroid Environment Near the Solar Ecliptic Plane. Paper presented at IAU/AIAA Symposium on Zodiacal Light and the Interplanetary Medium, Univ. Hawaii, Honolulu, Jan. 30-Feb. 2, 1967.
10. Wyatt, Stanley P., Jr.; and Whipple, Fred L.: The Poynting-Robertson Effect on Meteor Orbits. *Astrophys. J.*, vol. 111, Jan. 1950, pp. 134-141.
11. Jacchia, Luigi G.: The Physical Theory of Meteors. VIII. Fragmentation as Cause of the Faint-Meteor Anomaly. *Astrophys. J.*, vol. 121, no. 2, Mar. 1955, pp. 521-527.
12. Jacchia, Luigi G.: On Two Parameters Used in the Physical Theory of Meteors. *Smithsonian Contributions to Astrophysics*, vol. 2, no. 9, 1958, pp. 181-187.
13. Whipple, Fred L.: On Meteoroids and Penetration. *Smithsonian Astrophysical Observatory*, 1963.

14. Hawkins, Gerald S.; and Southworth, Richard B.: The Statistics of Meteors in the Earth's Atmosphere. Smithsonian Contributions to Astrophysics, vol. 2, no. 11, 1958, pp. 349-364.
15. Verniani, Franco: On the Luminous Efficiency of Meteors. Special Rep. No. 145, Smithsonian Astrophysical Observatory (NASA CR-55904), Feb. 17, 1964.
16. Jacchia, Luigi G.; Verniani, Franco; and Briggs, Robert E.: An Analysis of the Atmospheric Trajectories of 413 Precisely Reduced Photographic Meteors. Special Rep. No. 175, Smithsonian Inst. Astrophysical Observatory, Apr. 23, 1965.
17. Hawkins, Gerald S.; and Upton, Edward K.L.: The Influx Rate of Meteors in the Earth's Atmosphere. Astrophys. J., vol. 128, no. 3, Nov. 1958, pp. 727-735.
18. Kresák, L.: A Relation Between the Orbits and Magnitude Distribution of Meteors. Bull. Astronom. Inst. Czech., vol. 15, no. 5, 1964, pp. 190-201.
19. Dohnanyi, J. S.: Mass Distribution of Meteors. Astrophys. J., vol. 149, no. 3, Sept. 1967, pp. 735-737.
20. Erickson, James E.: Velocity Distribution of Sporadic Photographic Meteors. J. Geophys. Res., vol. 73, no. 12, June 15, 1968, pp. 3721-3726.
21. Dohnanyi, J. S.: Model Distribution of Photographic Meteors. Tech. Rep. 66-340-1, Bellcomm, Inc., Mar. 29, 1966.
22. Knip, Gerald Jr.; and Zola, Charles L.: Three-Dimensional Sphere-of-Influence Analysis of Interplanetary Trajectories to Mars. NASA TN D-1199, 1962.

FIRST CLASS MAIL

POSTMASTER: If Undeliverable (Section 158
Postal Manual) Do Not Return

"The aeronautical and space activities of the United States shall be conducted so as to contribute . . . to the expansion of human knowledge of phenomena in the atmosphere and space. The Administration shall provide for the widest practicable and appropriate dissemination of information concerning its activities and the results thereof."

— NATIONAL AERONAUTICS AND SPACE ACT OF 1958

NASA SCIENTIFIC AND TECHNICAL PUBLICATIONS

TECHNICAL REPORTS: Scientific and technical information considered important, complete, and a lasting contribution to existing knowledge.

TECHNICAL NOTES: Information less broad in scope but nevertheless of importance as a contribution to existing knowledge.

TECHNICAL MEMORANDUMS: Information receiving limited distribution because of preliminary data, security classification, or other reasons.

CONTRACTOR REPORTS: Scientific and technical information generated under a NASA contract or grant and considered an important contribution to existing knowledge.

TECHNICAL TRANSLATIONS: Information published in a foreign language considered to merit NASA distribution in English.

SPECIAL PUBLICATIONS: Information derived from or of value to NASA activities. Publications include conference proceedings, monographs, data compilations, handbooks, sourcebooks, and special bibliographies.

TECHNOLOGY UTILIZATION PUBLICATIONS: Information on technology used by NASA that may be of particular interest in commercial and other non-aerospace applications. Publications include Tech Briefs, Technology Utilization Reports and Notes, and Technology Surveys.

Details on the availability of these publications may be obtained from:

**SCIENTIFIC AND TECHNICAL INFORMATION DIVISION
NATIONAL AERONAUTICS AND SPACE ADMINISTRATION
Washington, D.C. 20546**